




Precision Measurement of Net-proton Number Fluctuations in Au+Au Collisions at RHIC

Yifei Zhang (for the STAR Collaboration)

University of Science and Technology of China



Outline

- ◆ Introduction
 - ◆ Experimental analysis
 - ◆ Results from BES-II
 - ◆ Summary and outlook
- 



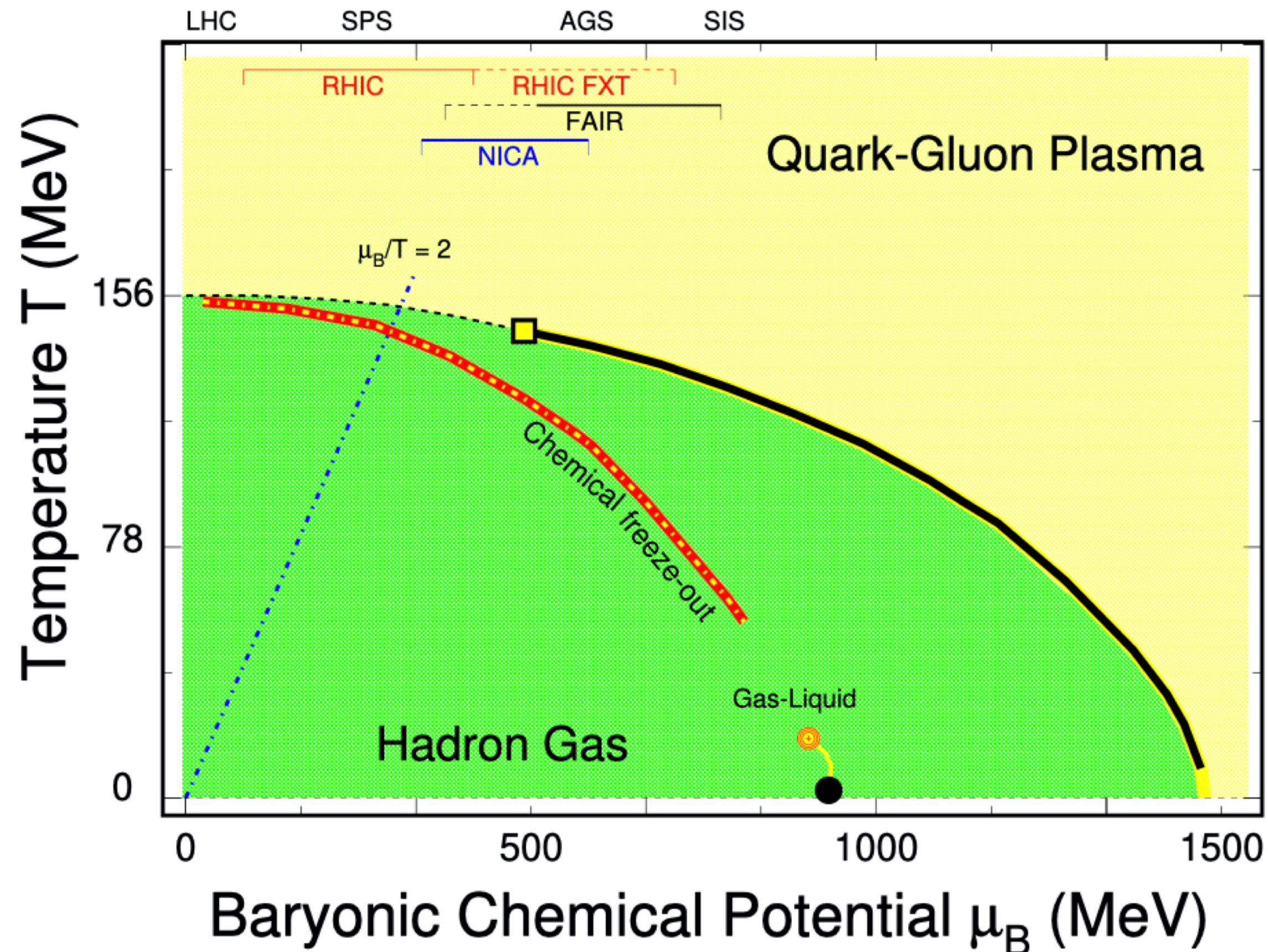
SOM 2024

The 21st International Conference on Strangeness in Quark Matter
3-7 June 2024, Strasbourg, France

SQM, June 6, 2024



Introduction: QCD Phase Diagram



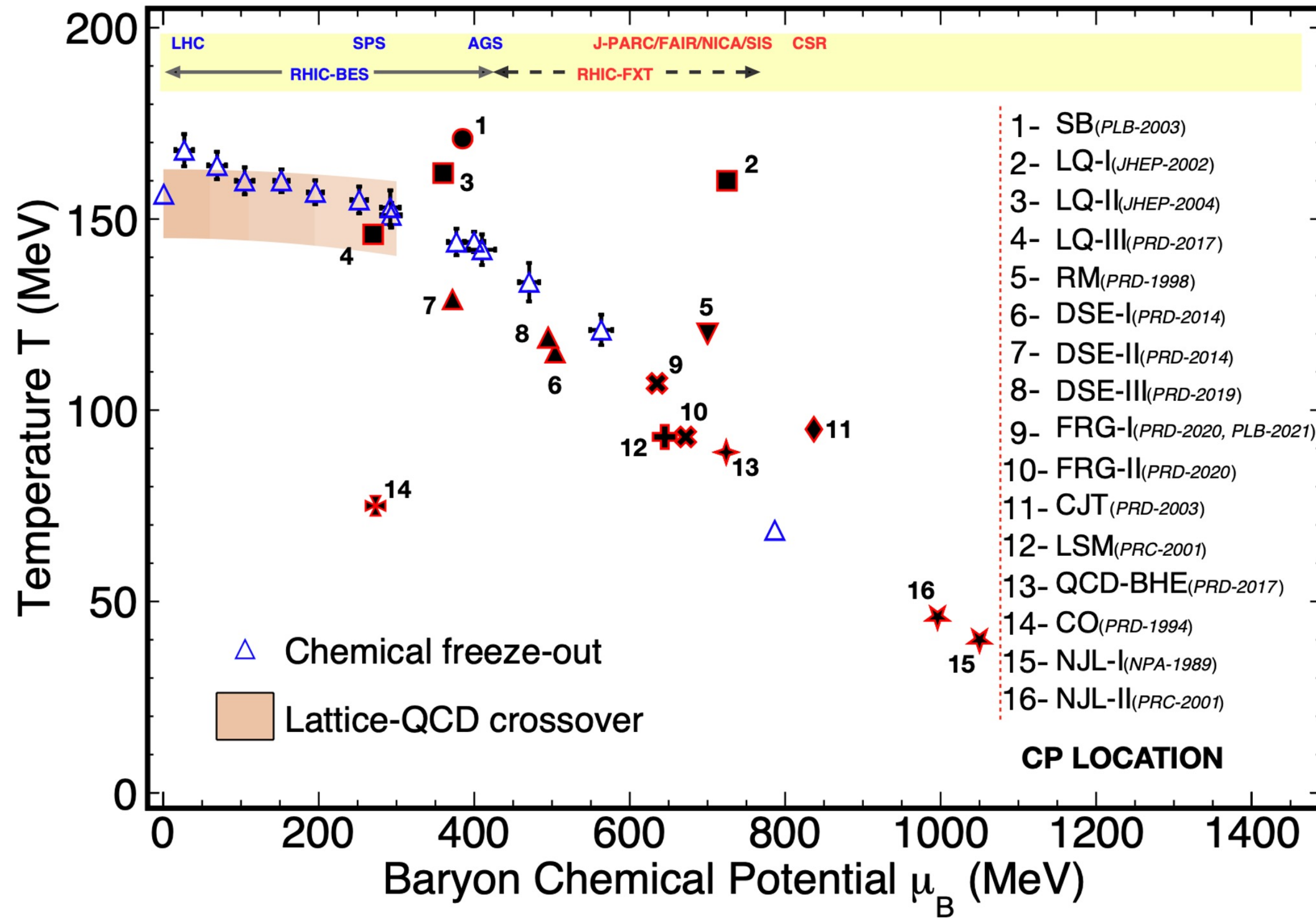
Phase diagram of strongly interacting matter

B. Mohanty, N. Xu, arXiv:2101.09210

Key features of phase structure:

- ◆ QGP and hadronic phase
- ◆ Crossover at small μ_B ($\frac{\mu_B}{T} < 2$) – compatible to all experimental observations.
- ◆ Transition temperature ($T_C \sim 156$ MeV) – Lattice QCD and verified by exp. chemical freeze-out.
- ◆ 1st order phase transition at large μ_B and **critical end point (CEP)** are conjectured.

Introduction: QCD Phase Diagram



A. Pandav, D. Mallick, B. Mohanty, PPNP. 125, 103960 (2022)

Key features of phase structure:

- QGP and hadronic phase
- Crossover at small μ_B ($\frac{\mu_B}{T} < 2$) – compatible to all experimental observations.
- Transition temperature ($T_C \sim 156$ MeV) – Lattice QCD and verified by exp. chemical freeze-out.
- 1st order phase transition at large μ_B and **critical end point (CEP)** are conjectured.

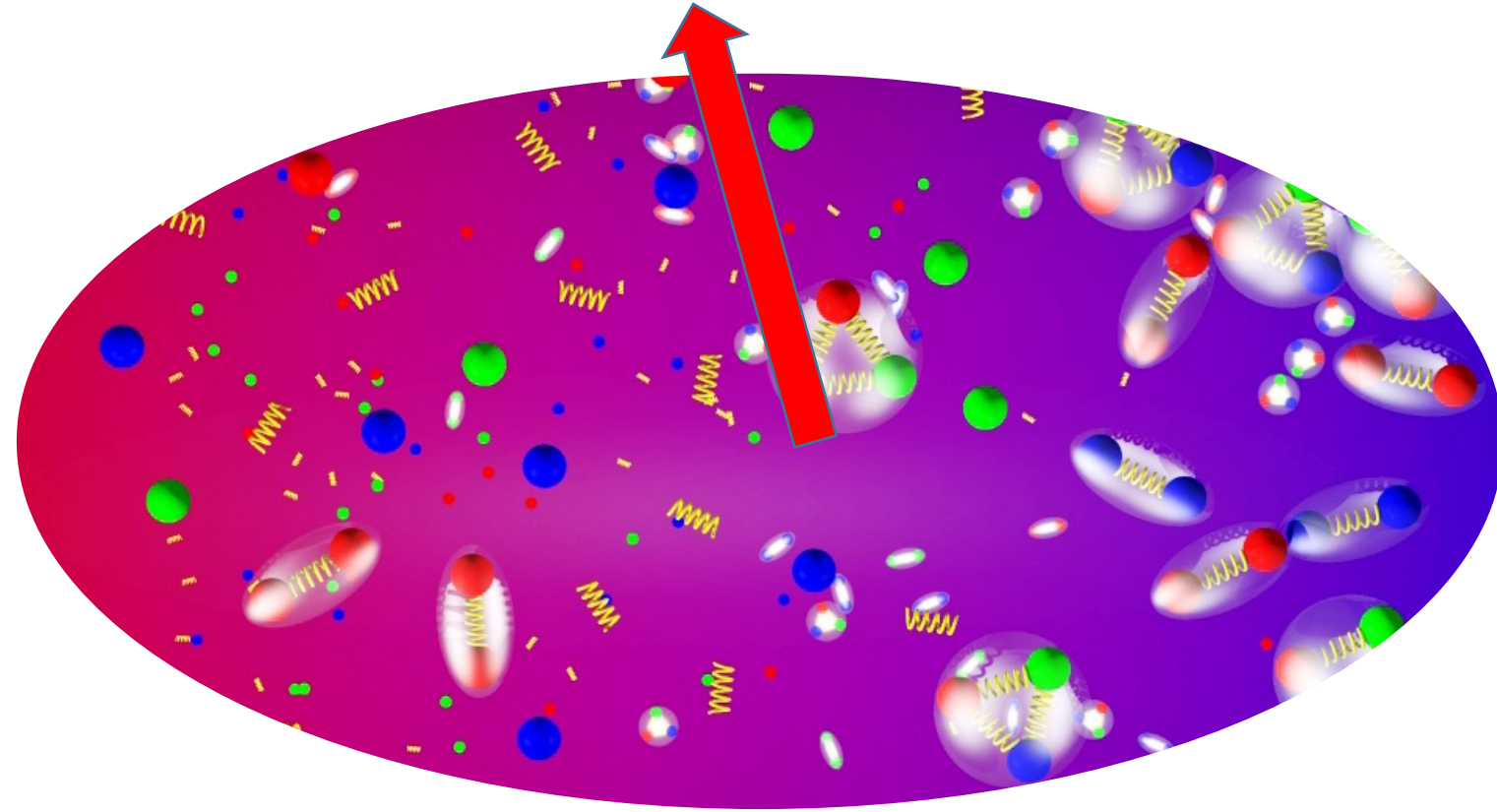
Sign problem in Lattice QCD at finite μ_B

Large uncertainties from models to locate the CEP.

Experimentally searching and locating CEP is crucial.

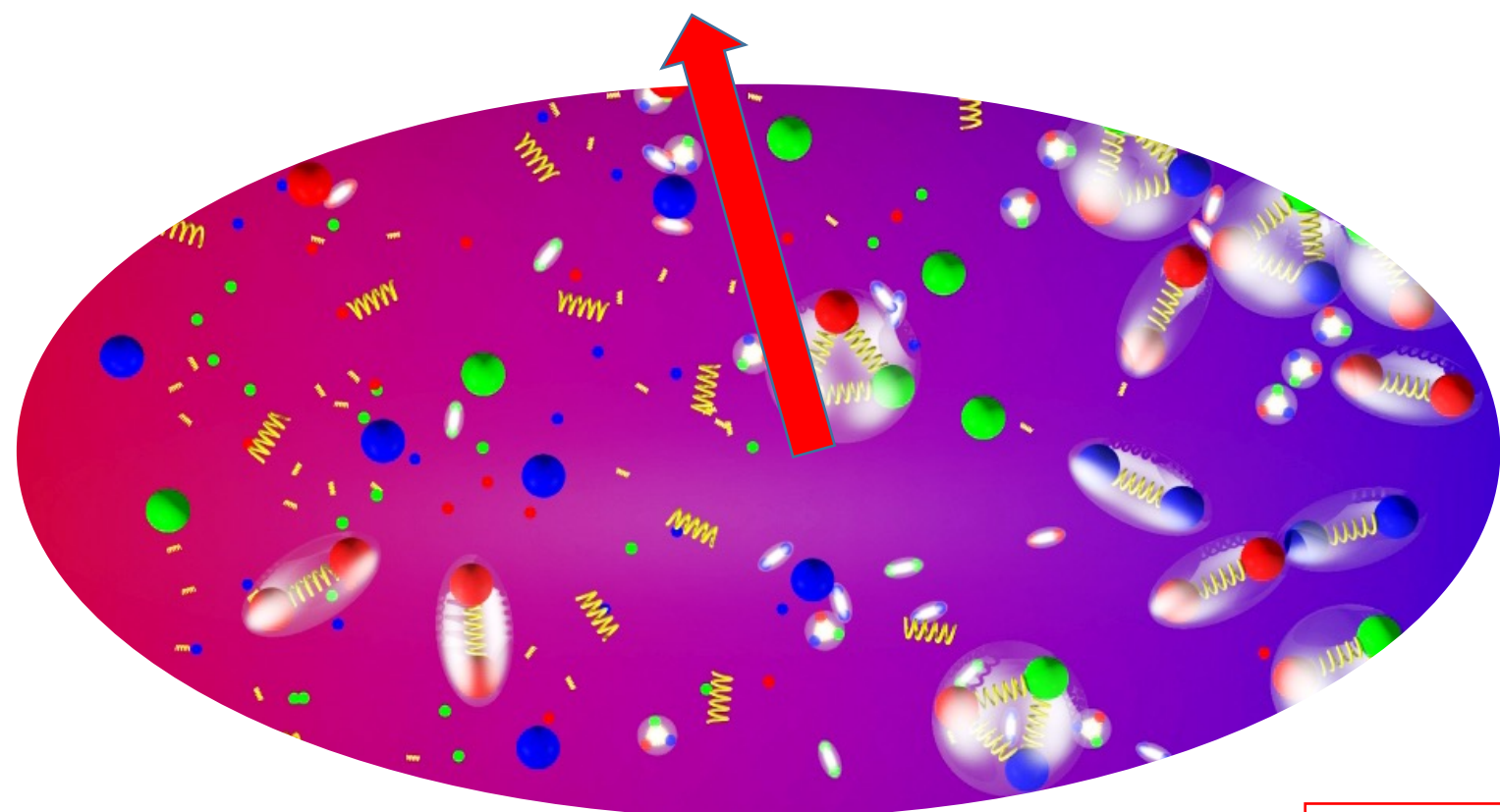
Introduction: Observables

At CEP: correlation length: ξ
susceptibilities: χ_n^q **expected to diverge**

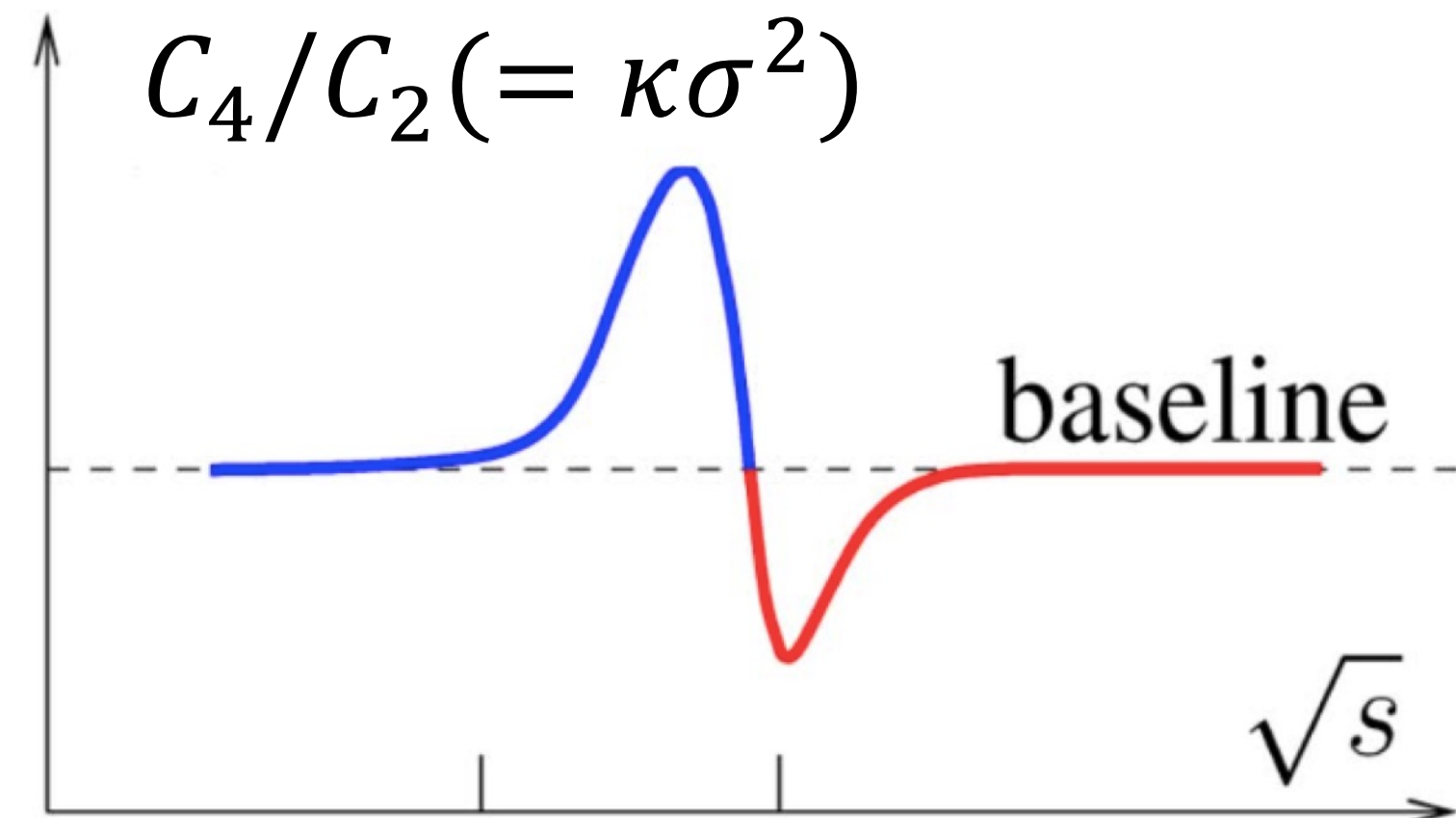


Introduction: Observables

At CEP: correlation length: ξ
susceptibilities: χ_n^q **expected to diverge**



CEP search



M. A. Stephanov, PRL 107 (2011) 052301

Assumption: Thermodynamic equilibrium

Non-monotonic energy dependence
of C_4/C_2 of conserved quantity -
existence of a critical region

$$C_2 \sim \xi^2, C_4 \sim \xi^7$$

$$\frac{C_{4q}}{C_{2q}} = \frac{\chi_4^q}{\chi_2^q}, \frac{C_{6q}}{C_{2q}} = \frac{\chi_6^q}{\chi_2^q}$$

$q = B, Q, S$

Allow the signal measurable

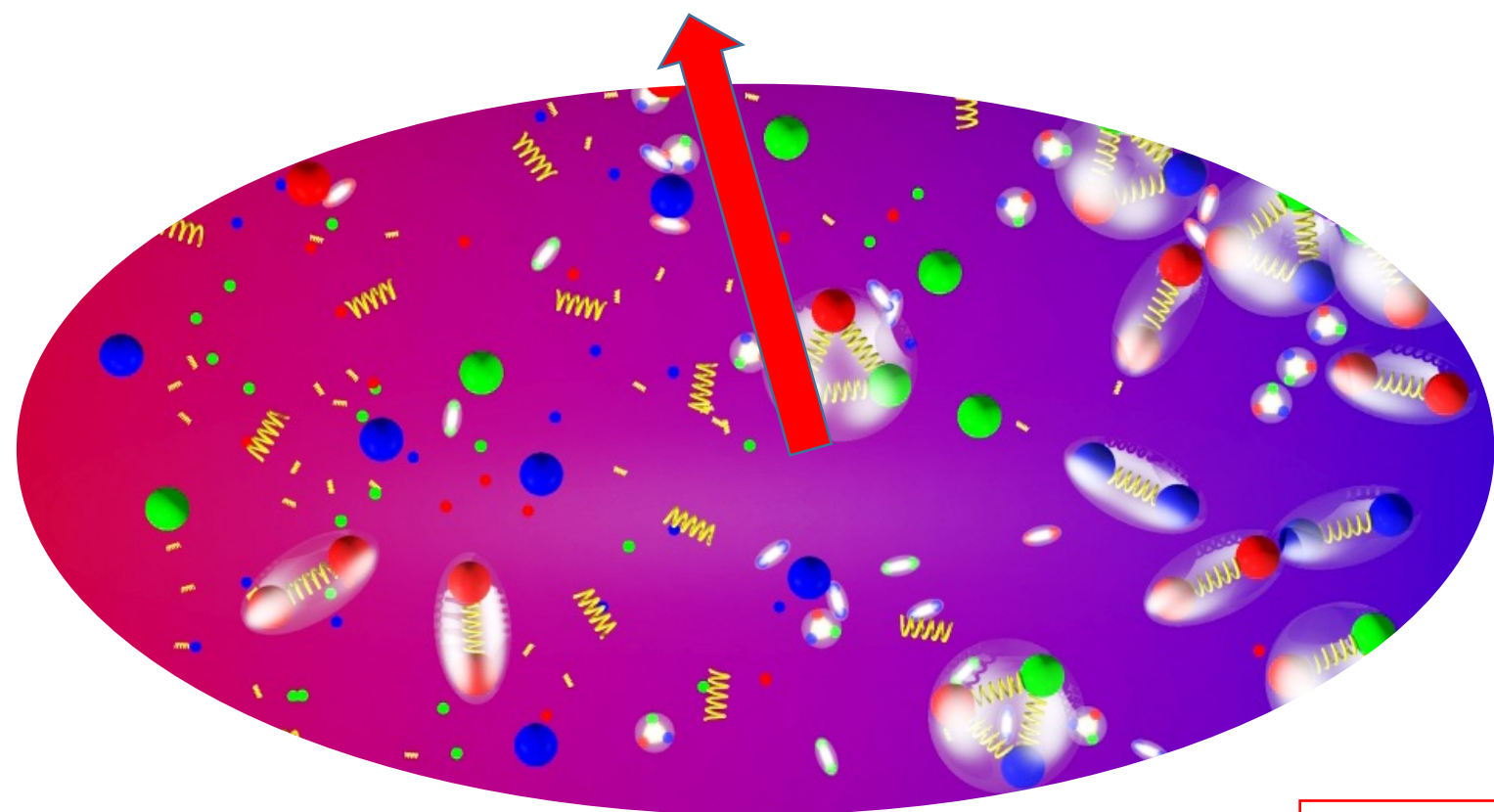
Finite size/time effects reduces ξ
Higher order \rightarrow more sensitivity

Direct comparison with lattice QCD,
HRG, QCD-based model calculations

R.V. Gavai and S. Gupta, PLB696, 459(11)
S. Ejiri, F. Karsch, K. Redlich, PLB633, 275(06)
A. Bazavov et al., PRL109, 192302(12)
S. Borsanyi et al., PRL111, 062005(13)

Introduction: Observables

At CEP: correlation length: ξ
susceptibilities: χ_n^q **expected to diverge**



Allow the signal measurable

Finite size/time effects reduces ξ
Higher order \longrightarrow more sensitivity

Direct comparison with lattice QCD,
HRG, QCD-based model calculations

$$C_2 \sim \xi^2, C_4 \sim \xi^7$$

$$\frac{C_{4q}}{C_{2q}} = \frac{\chi_4^q}{\chi_2^q}, \frac{C_{6q}}{C_{2q}} = \frac{\chi_6^q}{\chi_2^q}$$

$$q = B, Q, S$$

Cumulants

$n = E\text{-by-}E \text{ net-proton multiplicity}$

$$C_1 = \langle n \rangle$$

$$C_2 = \langle \delta n^2 \rangle \quad * \delta n = n - \langle n \rangle$$

$$C_3 = \langle \delta n^3 \rangle$$

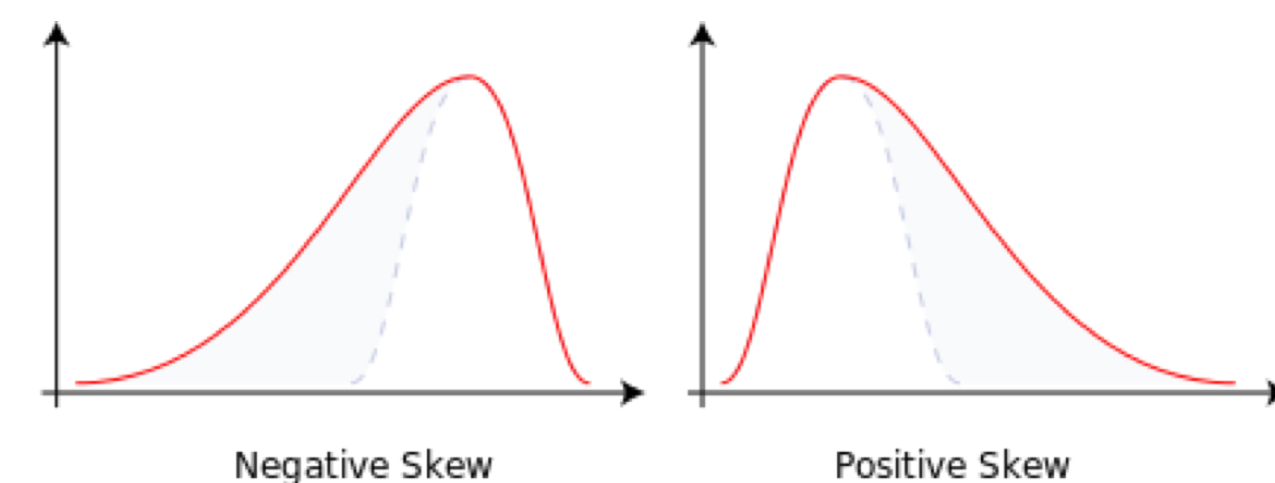
$$C_4 = \langle \delta n^4 \rangle - 3 \langle \delta n^2 \rangle^2$$

$$C_5 = \langle \delta n^5 \rangle - 10 \langle \delta n^3 \rangle \langle \delta n^2 \rangle$$

$$C_6 = \langle \delta n^6 \rangle - 15 \langle \delta n^4 \rangle \langle \delta n^2 \rangle - 10 \langle \delta n^3 \rangle^2 + 30 \langle \delta n^2 \rangle^3$$

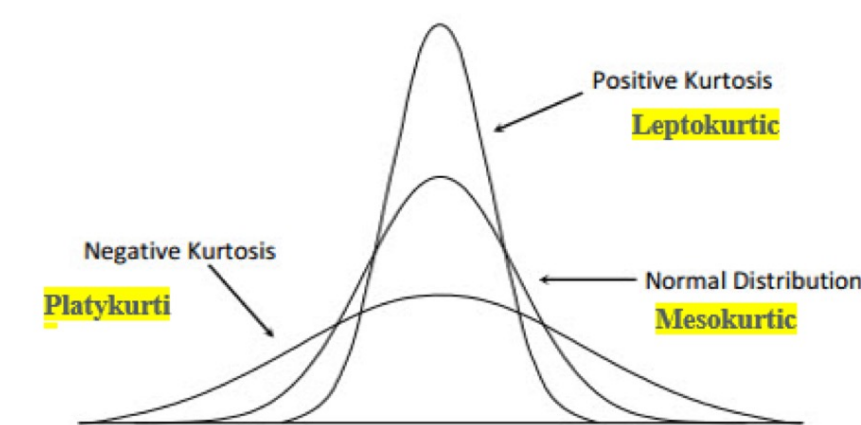
Skewness: Asymmetry

$$S = \langle (\delta N)^3 \rangle / \sigma^3 = C_3 / C_2^{3/2}$$



Kurtosis: Peakedness

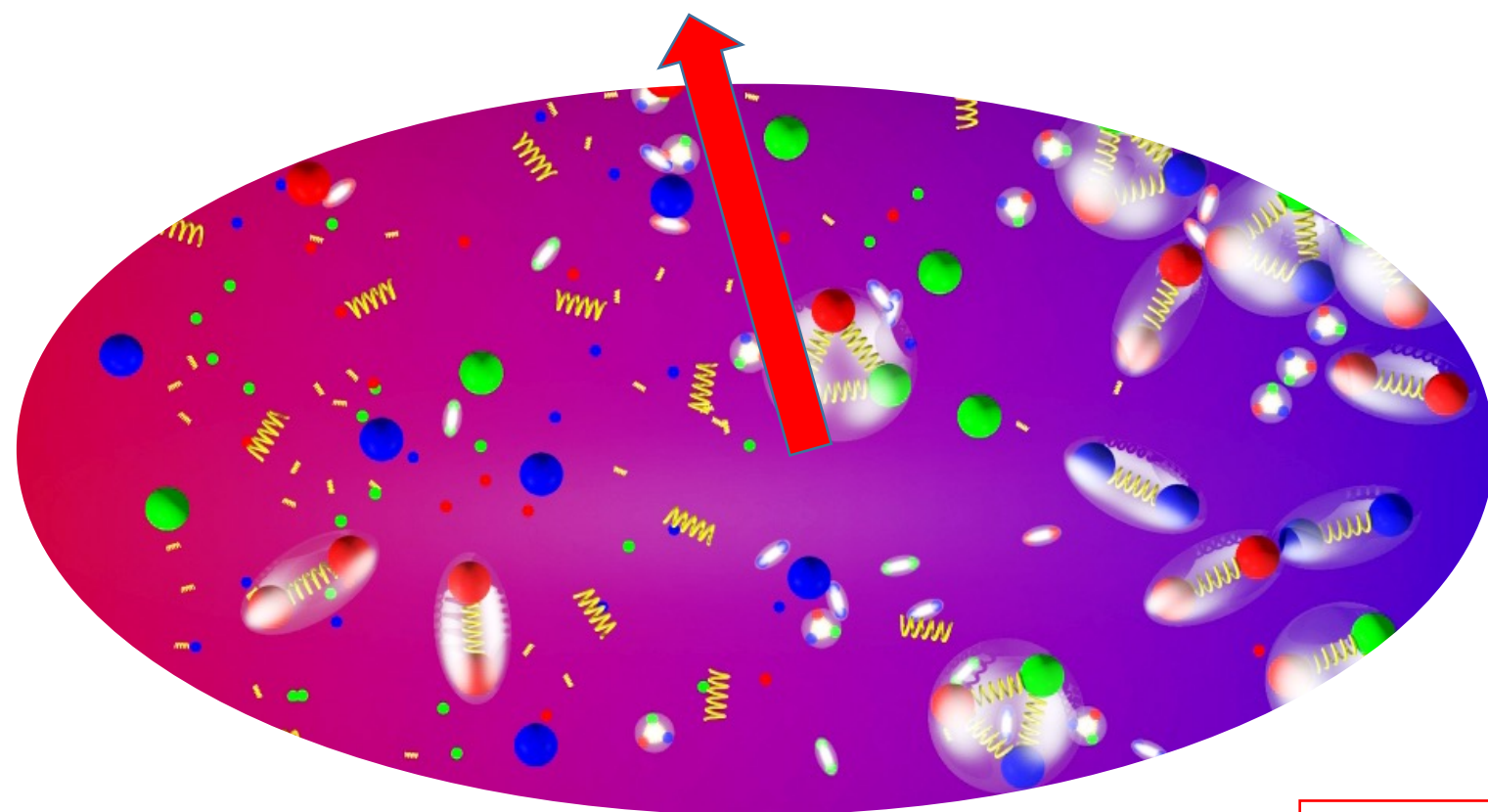
$$\kappa = \langle (\delta N)^4 \rangle / \sigma^4 - 3 = C_4 / C_2^2$$



R.V. Gavai and S. Gupta, PLB696, 459(11)
S. Ejiri, F. Karsch, K. Redlich, PLB633, 275(06)
A. Bazavov et al., PRL109, 192302(12)
S. Borsanyi et al., PRL111, 062005(13)

Introduction: Observables

At CEP: correlation length: ξ
susceptibilities: χ_n^q **expected to diverge**



Allow the signal measurable

- Finite size/time effects reduces ξ
Higher order \longrightarrow more sensitivity
- Direct comparison with lattice QCD,
HRG, QCD-based model calculations

$$C_2 \sim \xi^2, C_4 \sim \xi^7$$

$$\frac{C_{4q}}{C_{2q}} = \frac{\chi_4^q}{\chi_2^q}, \frac{C_{6q}}{C_{2q}} = \frac{\chi_6^q}{\chi_2^q}$$

$$q = B, Q, S$$

Cumulants

$n = E\text{-by-}E \text{ net-proton multiplicity}$

$$C_1 = \langle n \rangle$$

$$C_2 = \langle \delta n^2 \rangle \quad * \delta n = n - \langle n \rangle$$

$$C_3 = \langle \delta n^3 \rangle$$

$$C_4 = \langle \delta n^4 \rangle - 3 \langle \delta n^2 \rangle$$

$$C_5 = \langle \delta n^5 \rangle - 10 \langle \delta n^3 \rangle \langle \delta n^2 \rangle$$

$$C_6 = \langle \delta n^6 \rangle - 15 \langle \delta n^4 \rangle \langle \delta n^2 \rangle - 10 \langle \delta n^3 \rangle^2 + 30 \langle \delta n^2 \rangle^3$$

Factorial cumulants

$n = E\text{-by-}E \text{ (anti)proton multiplicity}$

$$\kappa_1 = C_1$$

$$\kappa_2 = -C_1 + C_2$$

$$\kappa_3 = 2C_1 - 3C_2 + C_3$$

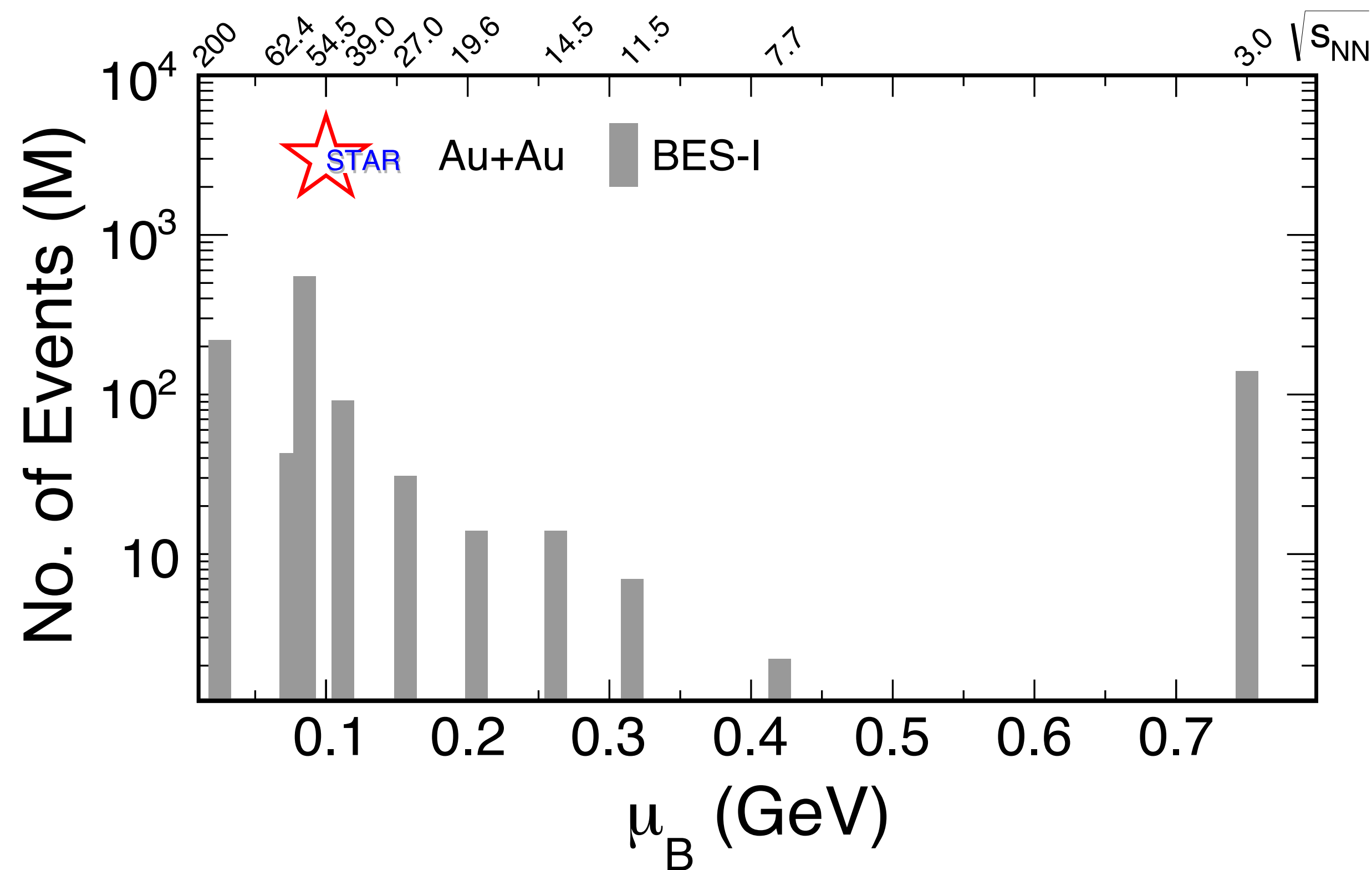
$$\kappa_4 = -6C_1 + 11C_2 - 6C_3 + C_4$$

$$\kappa_5 = 24C_1 - 50C_2 + 35C_3 - 10C_4 + C_5$$

$$\kappa_6 = -120C_1 + 274C_2 - 225C_3 + 85C_4 - 15C_5 + C_6$$

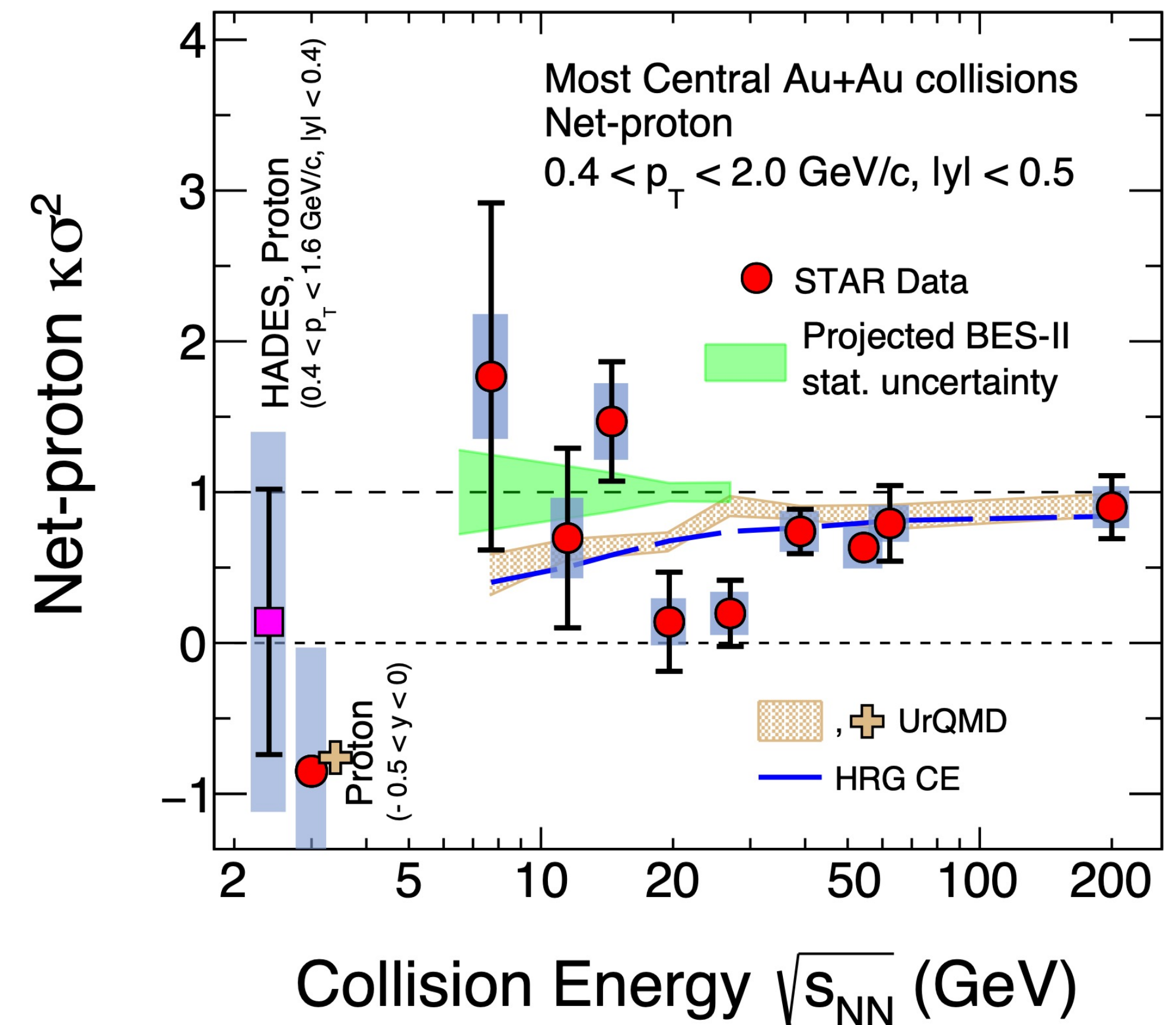
R.V. Gavai and S. Gupta, PLB696, 459(11)
S. Ejiri, F. Karsch, K. Redlich, PLB633, 275(06)
A. Bazavov et al., PRL109, 192302(12)
S. Borsanyi et al., PRL111, 062005(13)

Experimental Search for CEP from BES-I



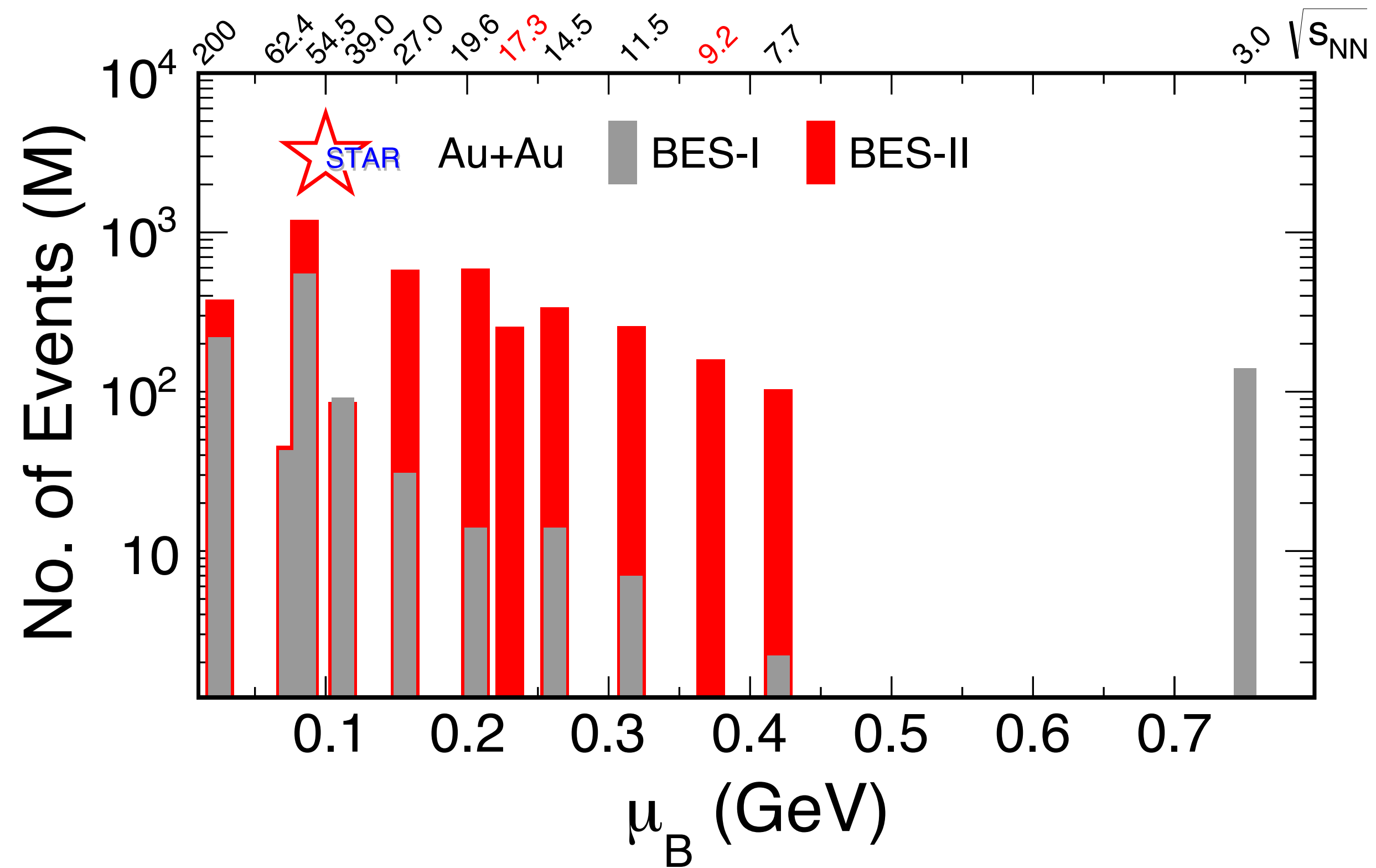
Phase I of BES program (BES-I)

STAR : PRL 127, 262301 (2021), PRC 104, 24902 (2021)
 : PRL 128, 202302 (2022), PRC 107, 24908 (2023)
 HADES: PRC 102, 024914 (2020)



- ◆ Non-monotonic distribution in central collisions from BES-I 200 to 7.7 GeV (3σ).
- ◆ Proton C_4/C_2 at 3 GeV with part of FXT data consistent with UrQMD.
- ◆ Non-CEP models with baryon conservation show a monotonic dependence vs. collision energy.

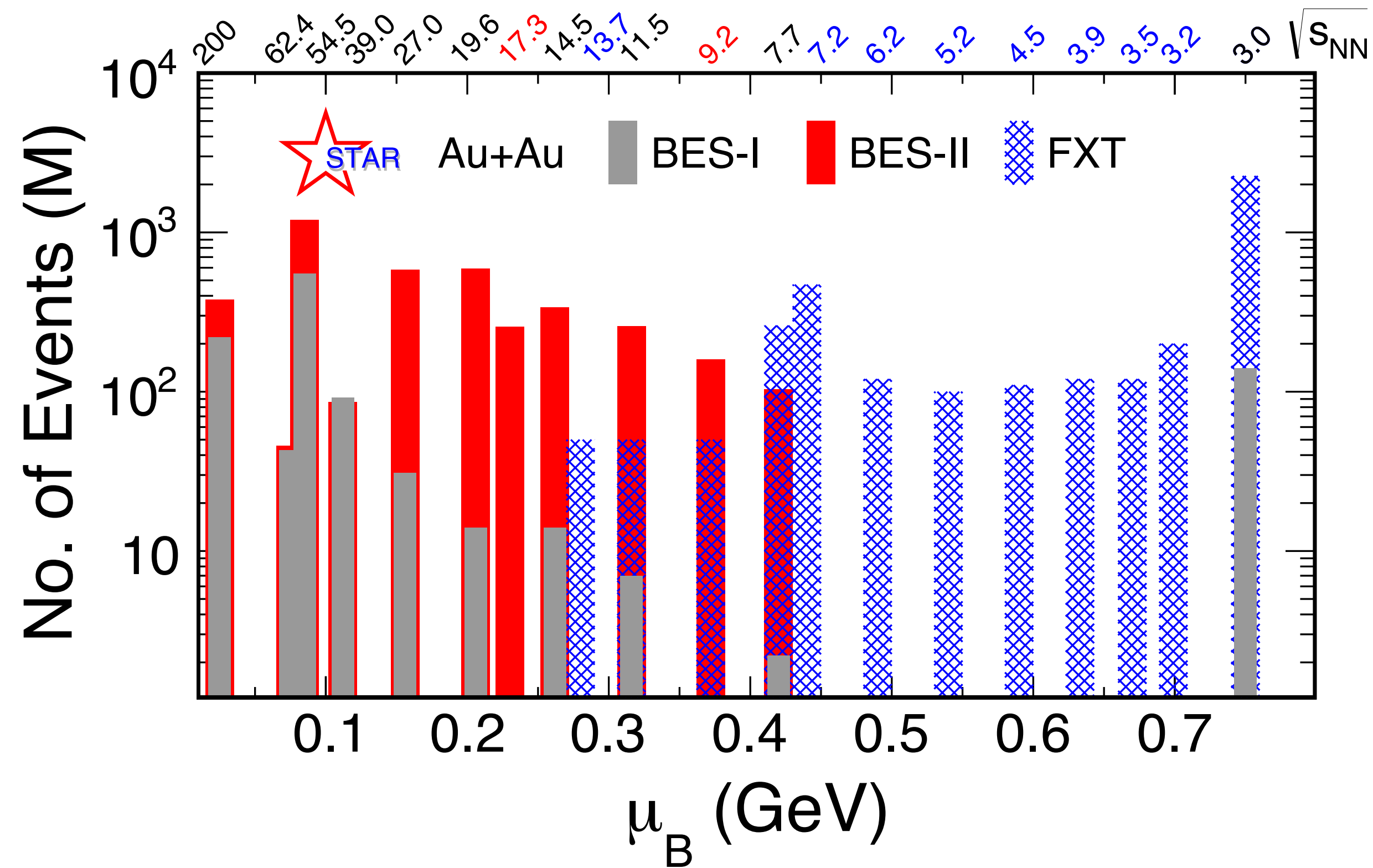
STAR BES-II program: Precision Measurement



Phase I of BES program (BES-I)

Phase II of BES program (BES-II) Collider mode

STAR BES-II program: Precision Measurement



Phase I of BES program (BES-I)

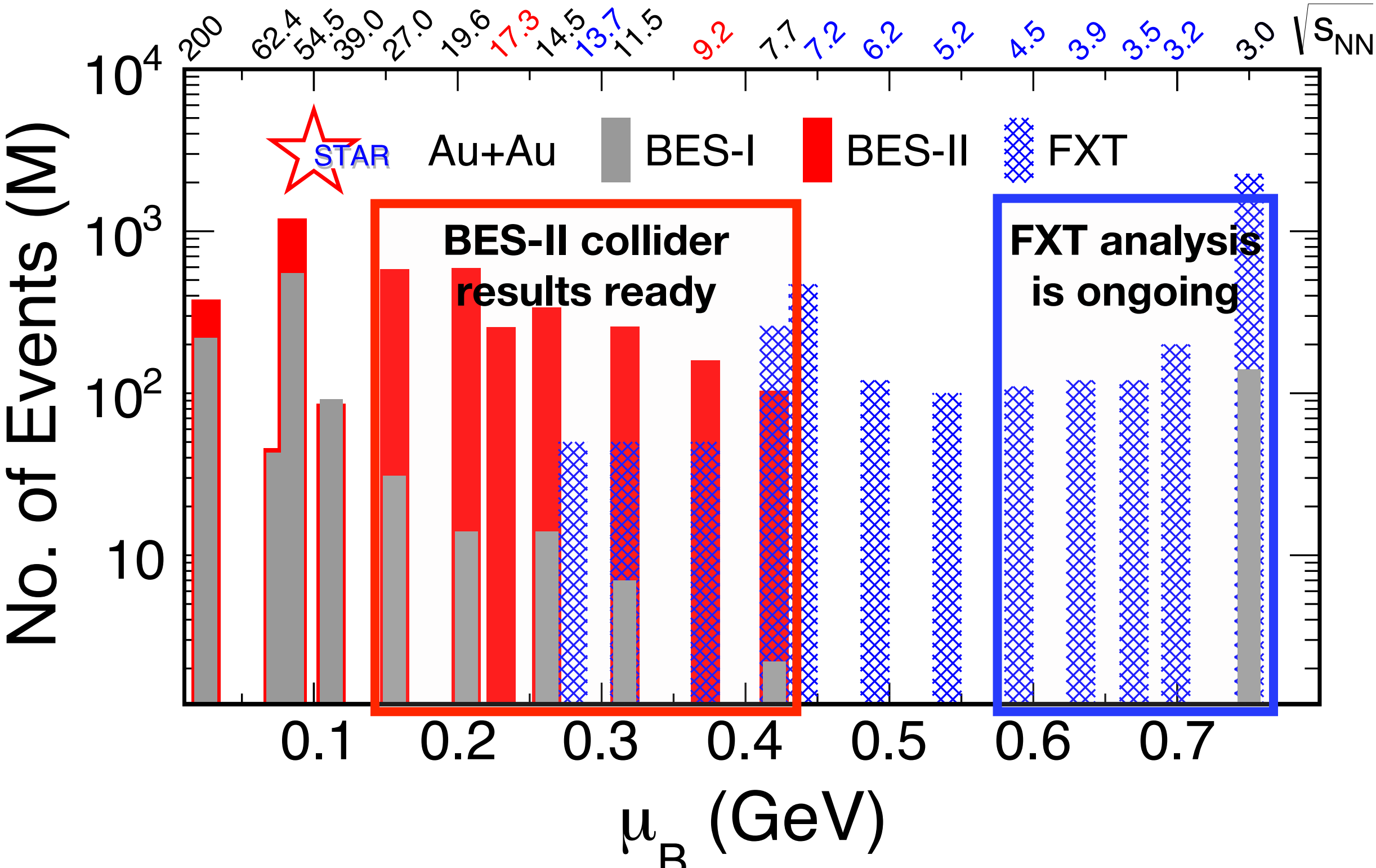
Phase II of BES program (BES-II) Collider mode

Fixed Target program (FXT)

$$3 \leq \sqrt{s_{NN}}(\text{GeV}) \leq 200 \rightarrow 750 \geq \mu_B(\text{MeV}) \geq 25$$

High precision, widest μ_B coverage to date

STAR BES-II program: Precision Measurement



Phase I of BES program (BES-I)

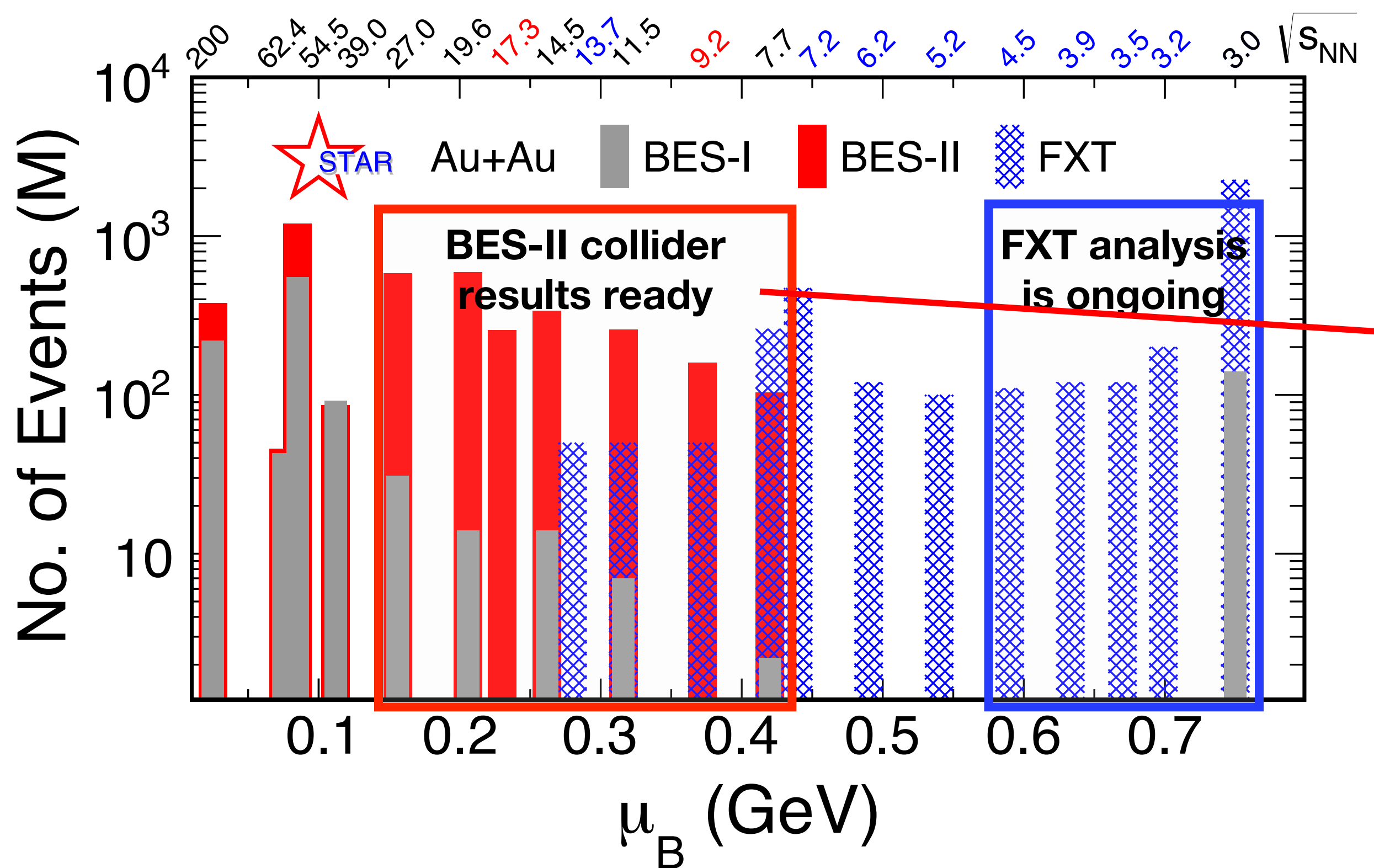
Phase II of BES program (BES-II) Collider mode

Fixed Target program (FXT)

$$3 \leq \sqrt{s_{NN}}(\text{GeV}) \leq 200 \rightarrow 750 \geq \mu_B(\text{MeV}) \geq 25$$

High precision, widest μ_B coverage to date

STAR BES-II program: Precision Measurement



Phase I of BES program (BES-I)

Phase II of BES program (BES-II)

Fixed Target program (FXT)

$$3 \leq \sqrt{s_{NN}}(\text{GeV}) \leq 200 \rightarrow 750 \geq \mu_B(\text{MeV}) \geq 25$$

Events used for net-proton fluctuation studies (Collider runs)

BES-II vs BES-I

$\sqrt{s_{NN}}$ (GeV)	Events BES-I (10 ⁶)	Events BES-II (10 ⁶)
7.7	3	45
9.2	-	78
11.5	7	110
14.5	20	178
17.3	-	116
19.6	15	270
27	30	220

~x10-18 larger statistics

9.2 and 17.3 GeV added to energy scan

High precision, widest μ_B coverage to date

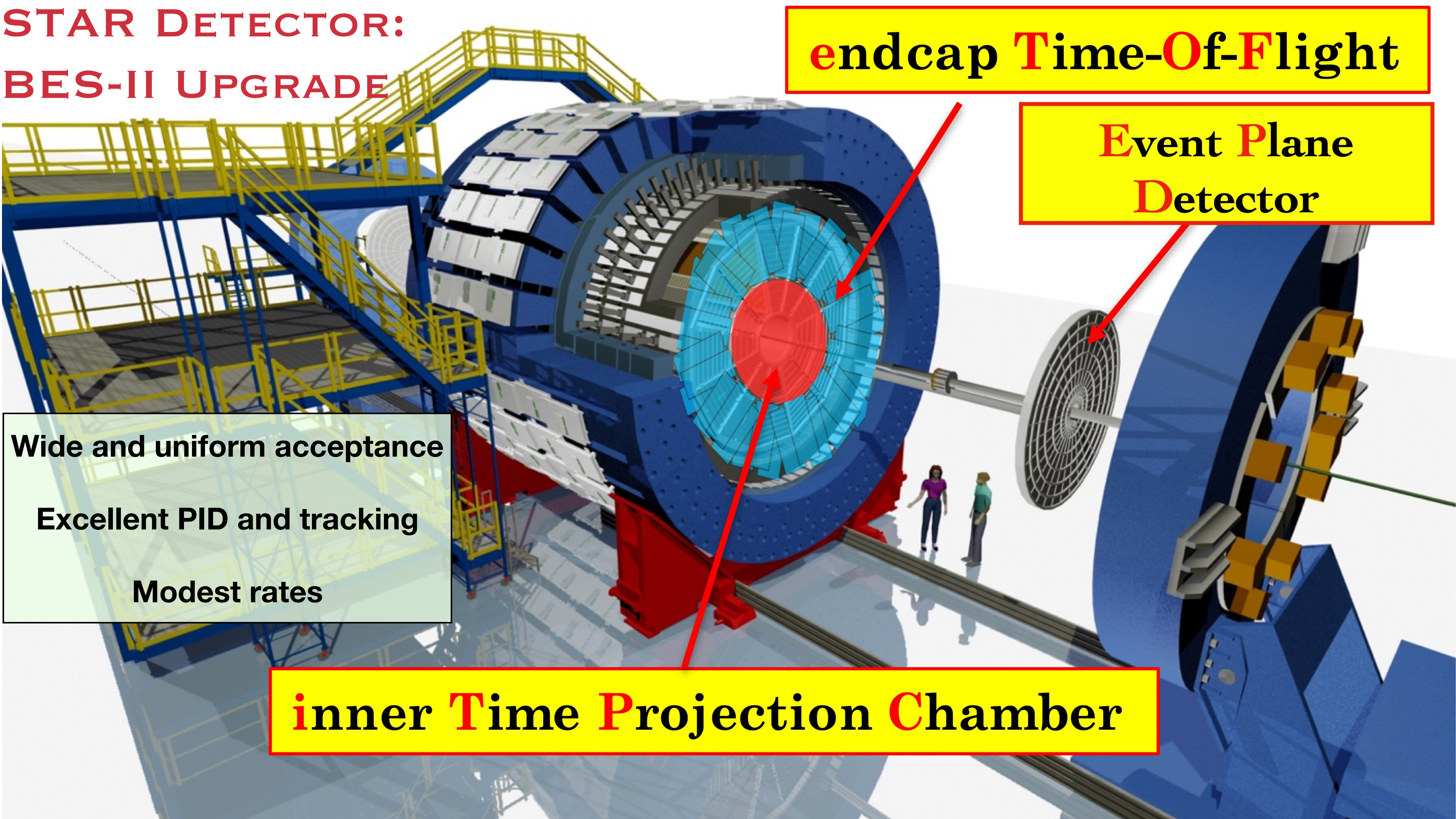
STAR DETECTOR: BES-II UPGRADE

endcap **T**ime-**O**f-**F**light

Event **P**lane
Detector

Wide and uniform acceptance
Excellent PID and tracking
Modest rates

inner **T**ime **P**rojection **C**hamber



STAR Major Upgrades for BES-II



iTPC:

- Improves dE/dx
- Extends η coverage from 1.0 to 1.6
- Lowers p_T cut-in from 125 to 60 MeV/c
- Ready in 2019

eTOF:

- Forward rapidity coverage
- PID at $\eta = 1.05$ to 1.5
- Borrowed from CBM-FAIR
- Ready in 2019

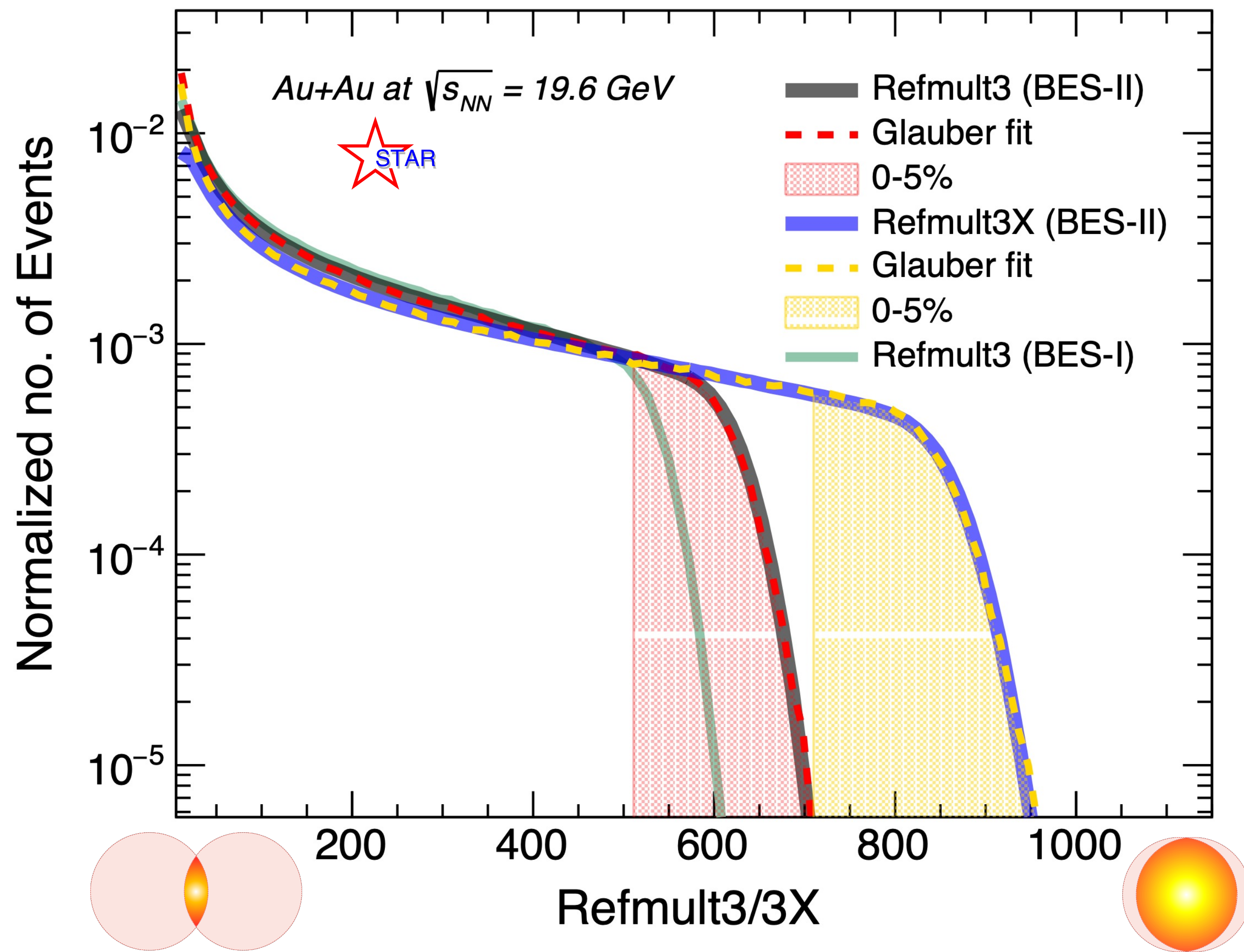
EPD:

- Improves trigger
- Better centrality & event plane measurements
- Ready in 2018

- 1) Enlarge rapidity acceptance: $|\eta| \leq 1.0 \rightarrow |\eta| \leq 1.6$
- 2) Improve particle identification: $p_T \geq 125 \text{ MeV}/c \rightarrow p_T \geq 60 \text{ MeV}/c$
- 3) Enhance centrality/event plane resolution, suppress auto correlations
- 4) Enable the fixed-target program: $\mu_B \leq 420 \text{ MeV} \rightarrow \mu_B \leq 750 \text{ MeV}$

Centrality Definition

- Defined using charged particle multiplicity measured by STAR
- Exclude protons and antiprotons to avoid self correlation



Two centrality definitions with different acceptance:

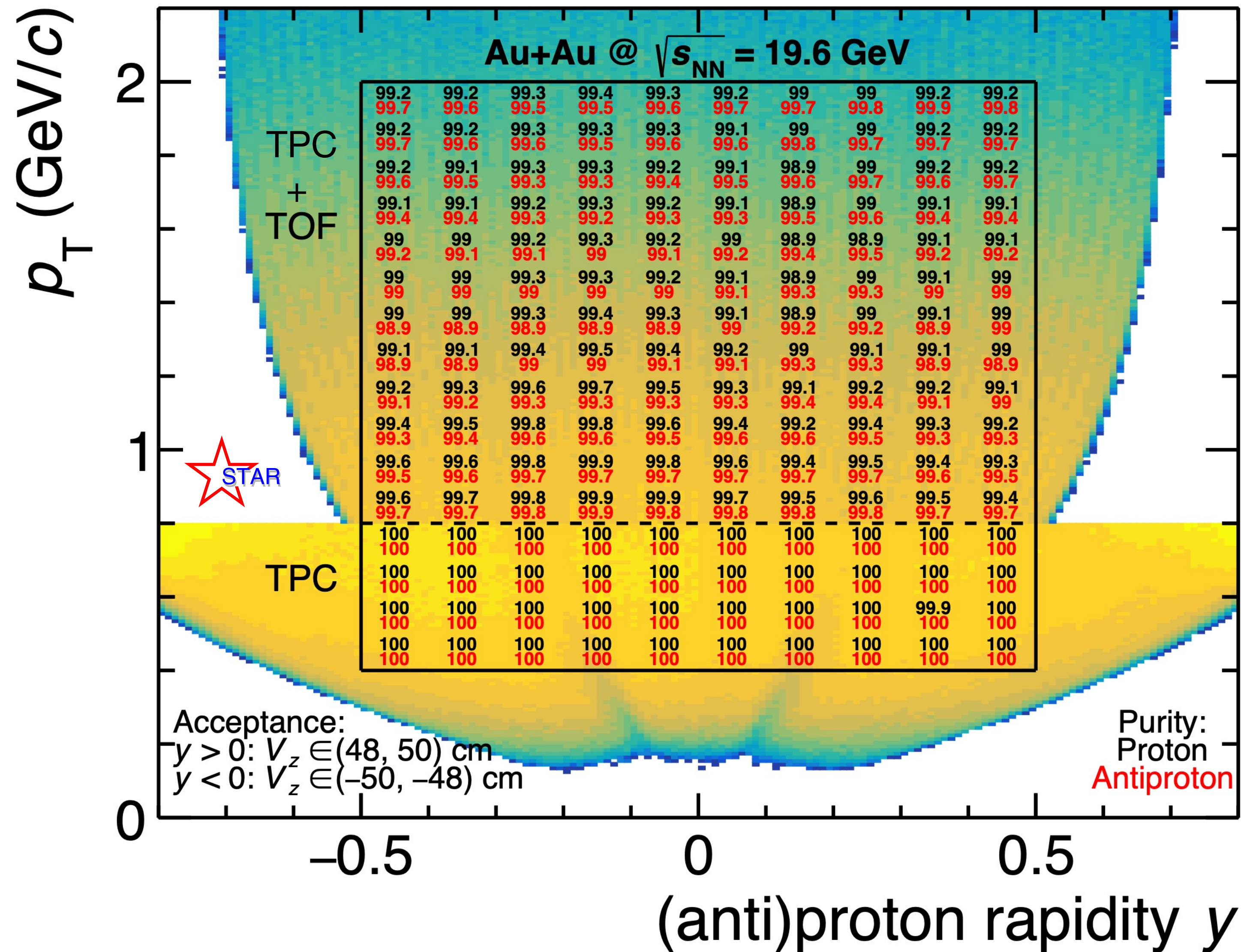
Refmult3		Refmult3X
Charged particle multiplicity excluding protons		
BES-I	BES-II	BES-II
w/o iTPC	w/ iTPC	w/ iTPC
$ \eta < 1.0$	$ \eta < 1.0$	$ \eta < 1.6$

Refmult3X (BES-II) > Refmult3 (BES-II) > Refmult3 (BES-I)



Best centrality resolution

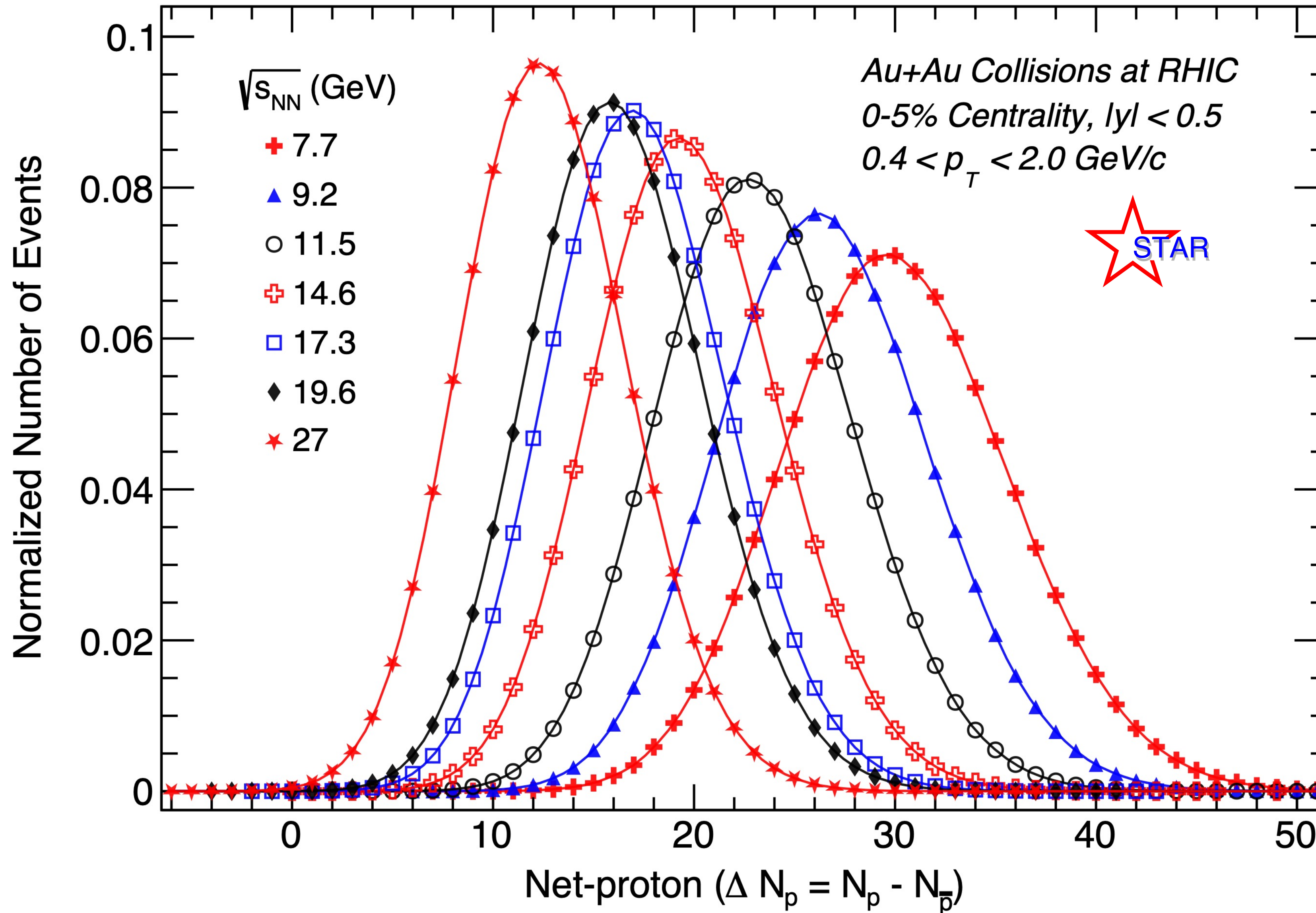
Proton Identification



p_T (GeV/c)	0.4 – 0.8	0.8 – 2.0
rapidity	$ y < 0.5$	
detector	TPC	TPC+TOF
dE/dx	$ n\sigma < 2$	
mass ² (GeV ² /c ⁴)	/	0.6 – 1.2

- ✦ Uniform acceptance for (anti-) protons $|y| < 0.5$ with $|V_z| < 50$ cm
- ✦ (anti-)protons identified using TPC dE/dx + TOF
- ✦ Bin-by-bin purity $> 99\%$ in the full acceptance range and all energies

Event-by-Event Net-proton Number Distribution



- Raw net-proton number distributions from BES-II: Uncorrected for detector efficiency
- Mean increases with decreasing collision energy: Effect of baryon stopping

Improved statistics and systematics

✦ Better statistics:

~x10 – 18 larger statistics compared with BES-I

$$\text{Stat. error } C_r \propto \frac{\sigma^r}{\sqrt{N}}$$

STAR, PRC 104 (2021) 024902

✦ Larger acceptance and improved tracking

Benefit from iTPC upgrade

~10% higher proton efficiency compared to BES-I

Better control on uncertainty on efficiency: 2% compared to 5% in BES-I

✦ Better centrality resolution

Corrected for finite centrality bin with event-number-weighted average

$$C_n = \sum_r w_r C_{n,r}$$

where $w_r = n_r / \sum_r n_r$, $n=1,2,3,4\dots$

Here, n_r is no. of events in r^{th} multiplicity bin

**Reduction factor in uncertainties on 0-5% C_4/C_2 :
BES-II vs BES-I**

7.7 GeV		19.6 GeV	
stat. error	sys. error	stat. error	sys. error
4.7	3.2	4.5	4

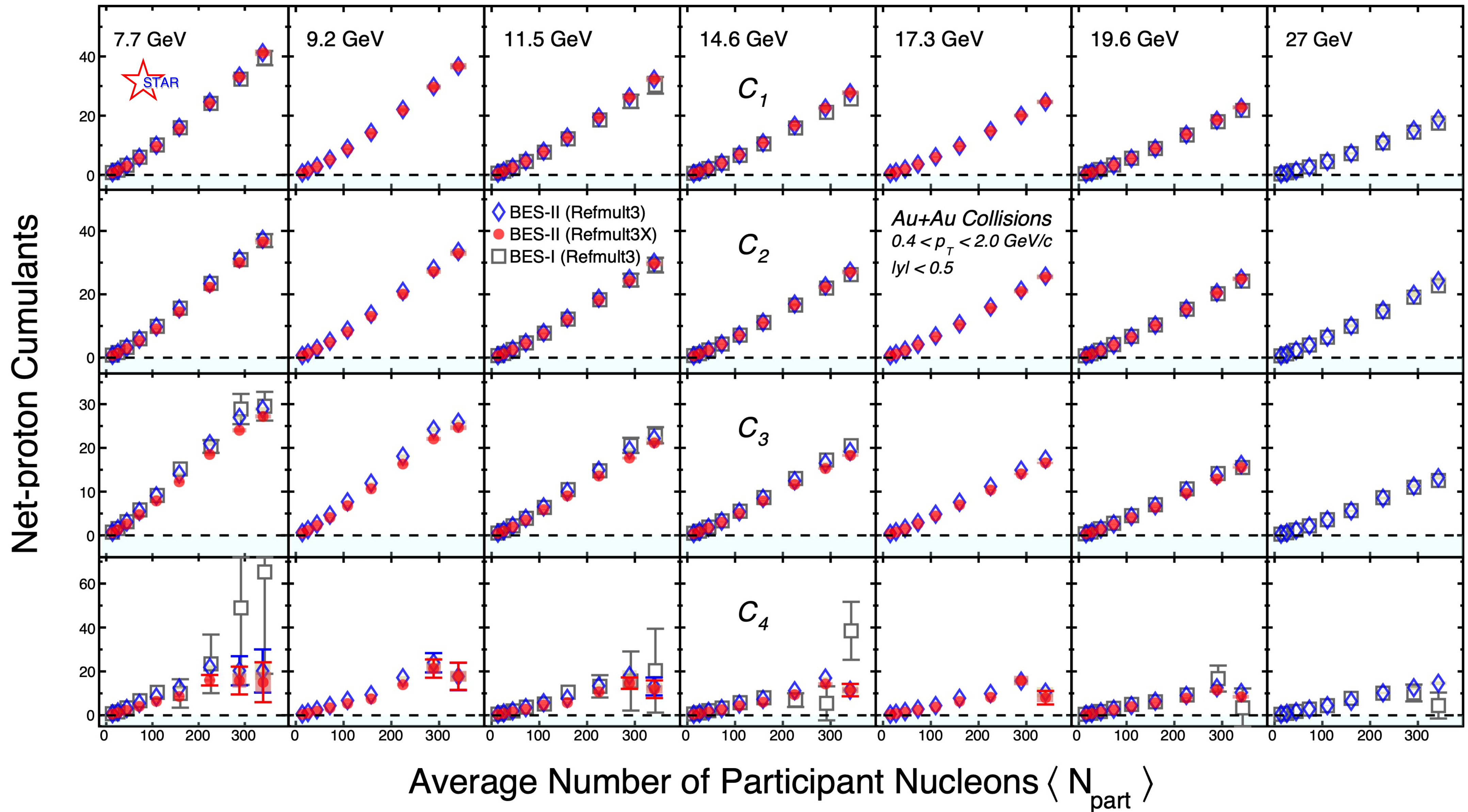
X. Luo, T Nonaka, PRC 99 (2019), X. Luo et al, J.Phys. G 40, 105104 (2013)



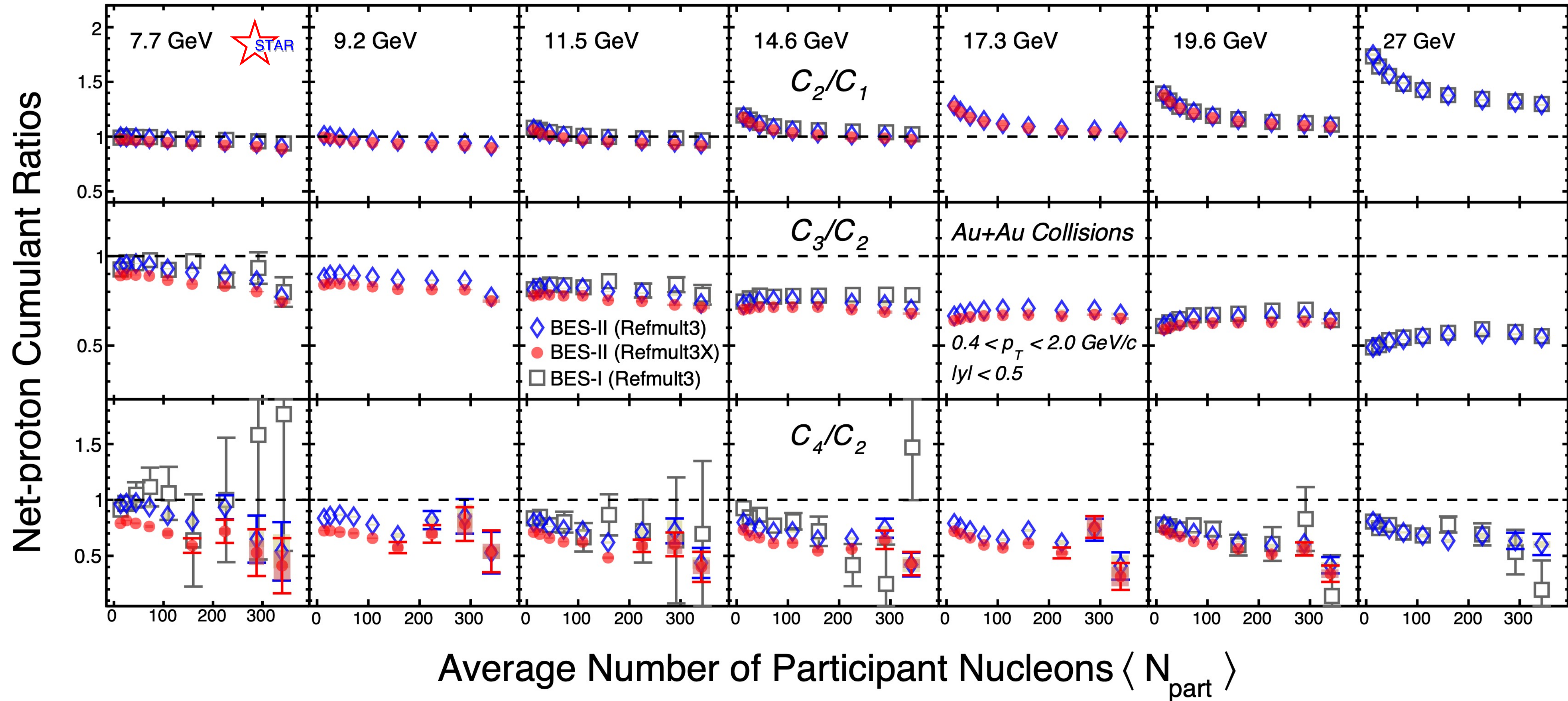
Latest Net-proton Fluctuation Results from STAR BES-II



Cumulants vs Centrality and Collision Energies

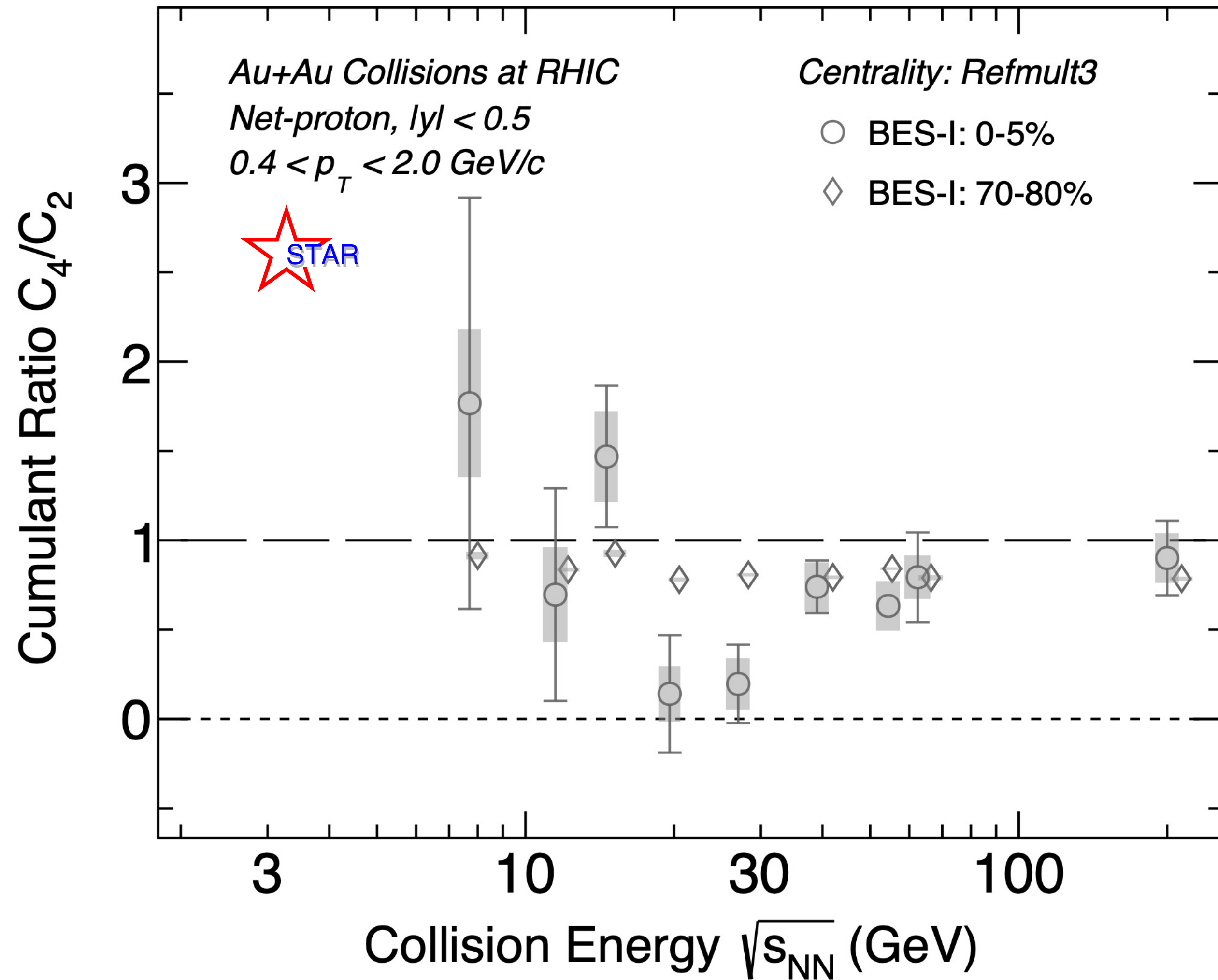


Cumulant ratios vs Centrality and Collision Energies

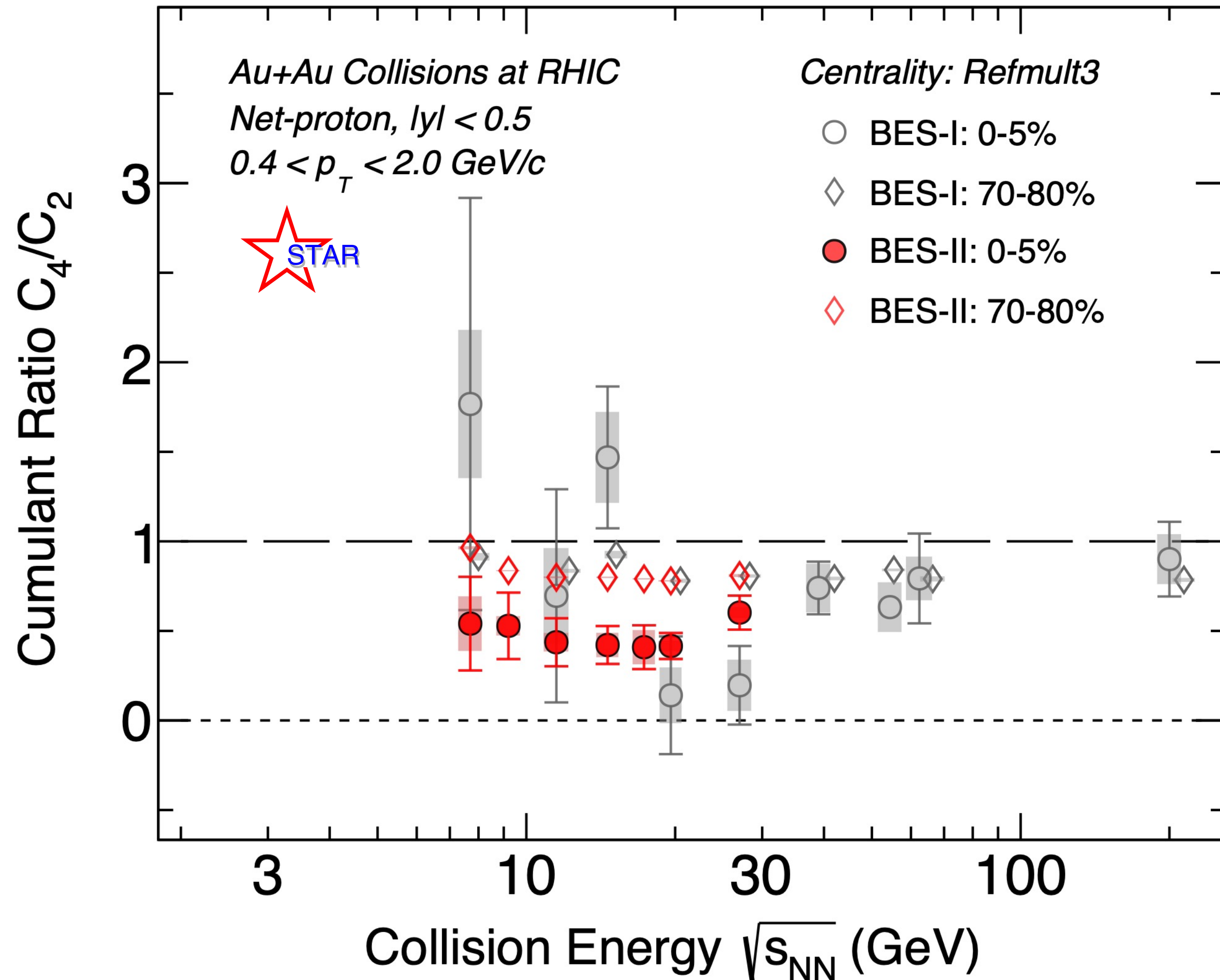


- ◆ Precision measurements: smooth variation across centrality and collision energy observed.
- ◆ Higher centrality resolution leads to lower ratios (especially in mid central and peripheral collisions):
Results from Refmult3X (BES-II) < Refmult3 (BES-II) < Refmult3 (BES-I)
- ◆ For 0-5% C_4/C_2 , weak effect of centrality resolution seen.

Energy Dependence of C_4/C_2 : Comparison with BES-I



Energy Dependence of C_4/C_2 : Comparison with BES-I

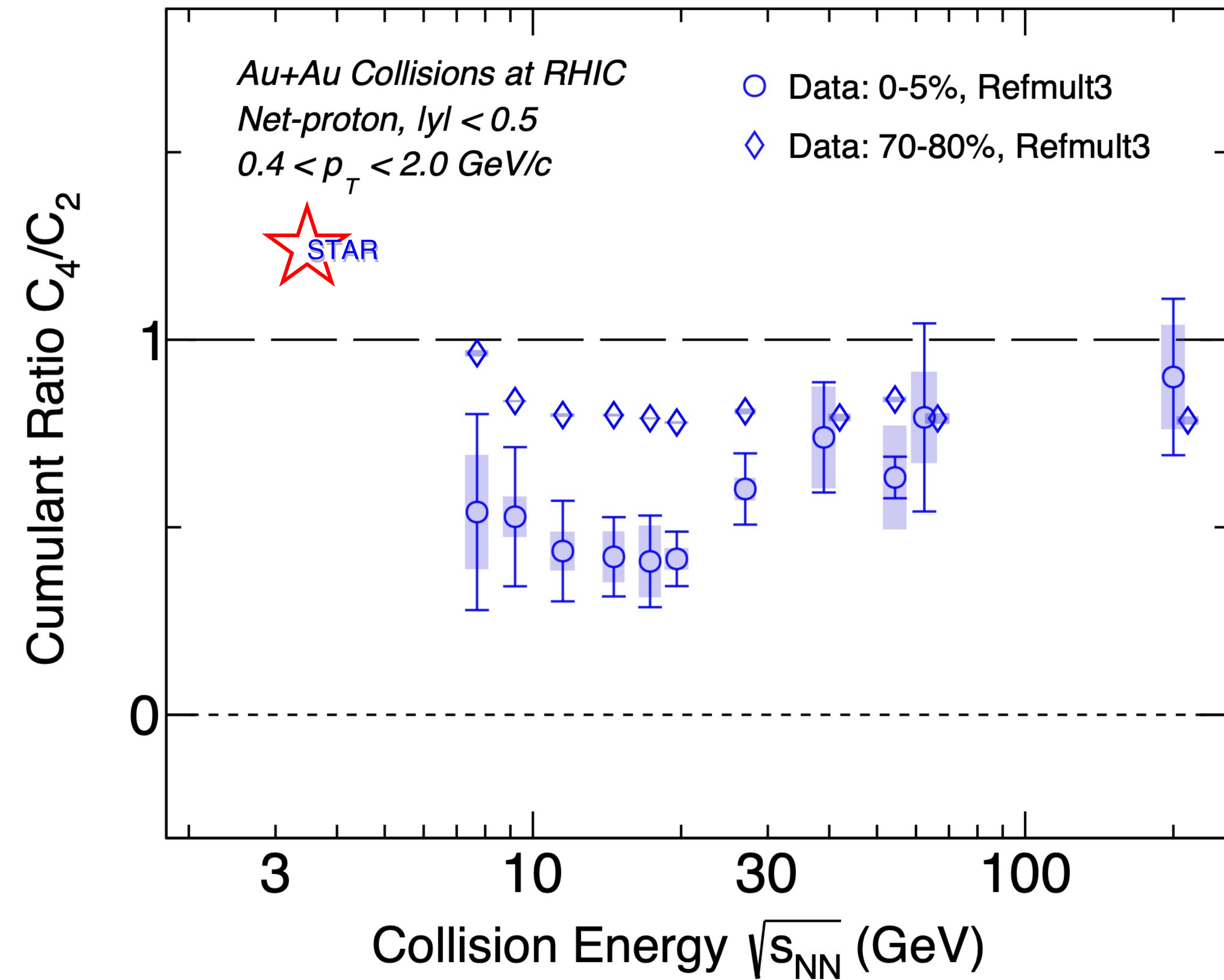


Deviation between BES-II and BES-I data

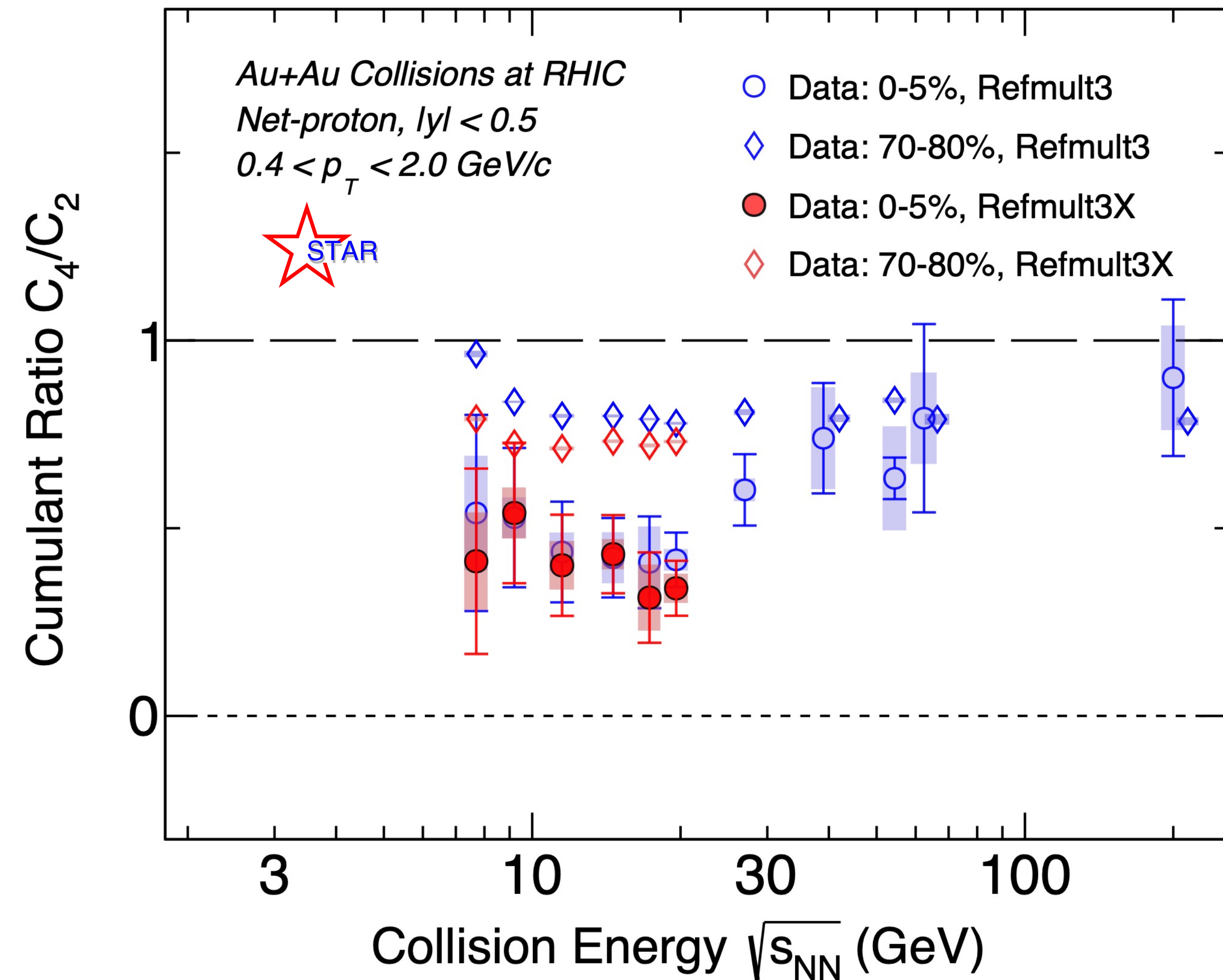
$\sqrt{s_{NN}}$ (GeV)	0-5%	70-80%
7.7	1.0 σ	0.9 σ
11.5	0.4 σ	1.3 σ
14.6	2.2 σ	2.5 σ
19.6	0.7 σ	0.0 σ
27	1.4 σ	0.2 σ

◆ BES-II results consistent with BES-I within uncertainties.

Effect of Centrality Resolution on C_4/C_2



Effect of Centrality Resolution on C_4/C_2



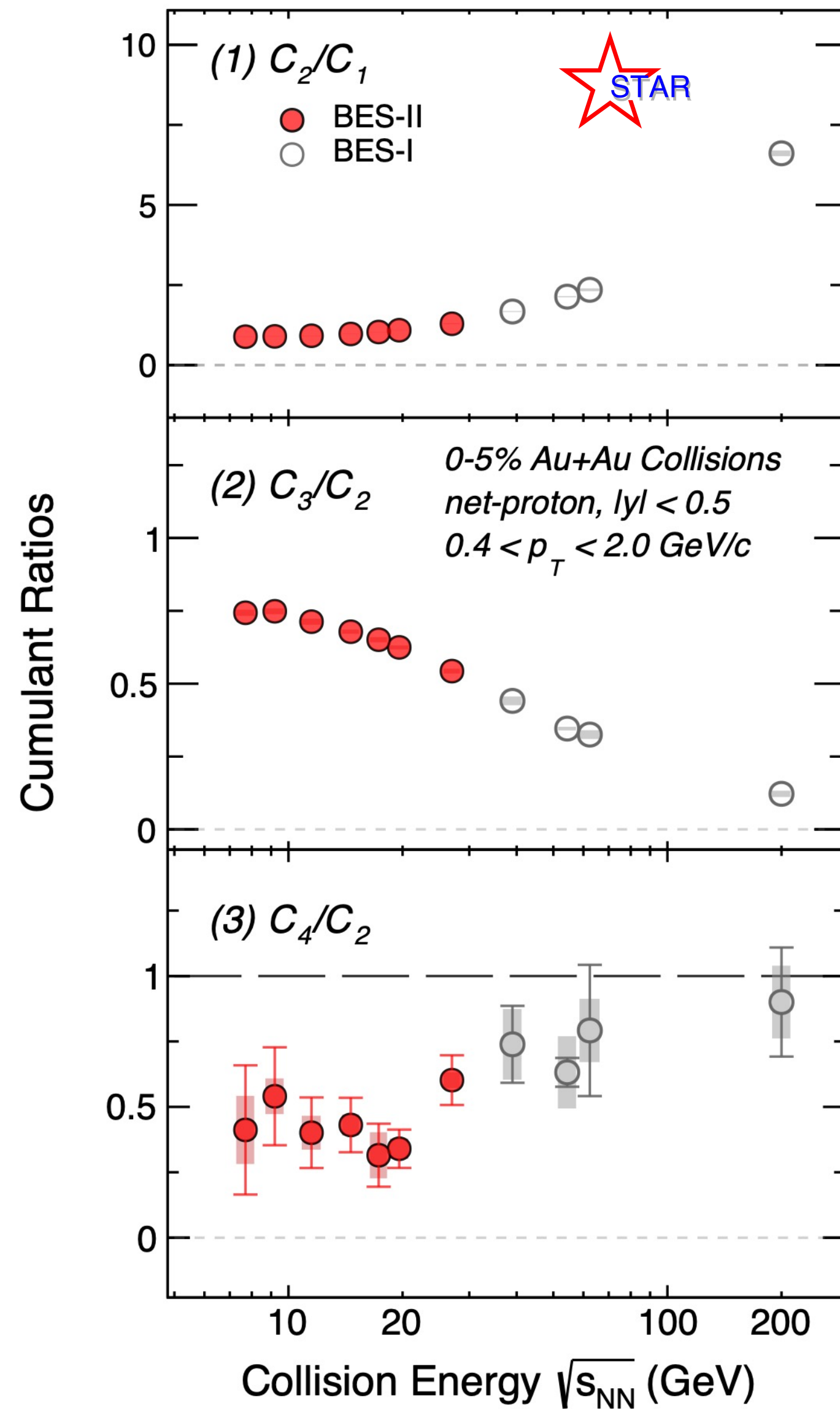
◆ 0–5% centrality C_4/C_2 results show good agreement between Refmult3 and Refmult3X: **weak effect of centrality resolution.**

◆ Difference in 70–80% due to centrality resolution impact.

BES-II results shown hereafter are with Refmult3X

Energy Dependence: Model Comparison

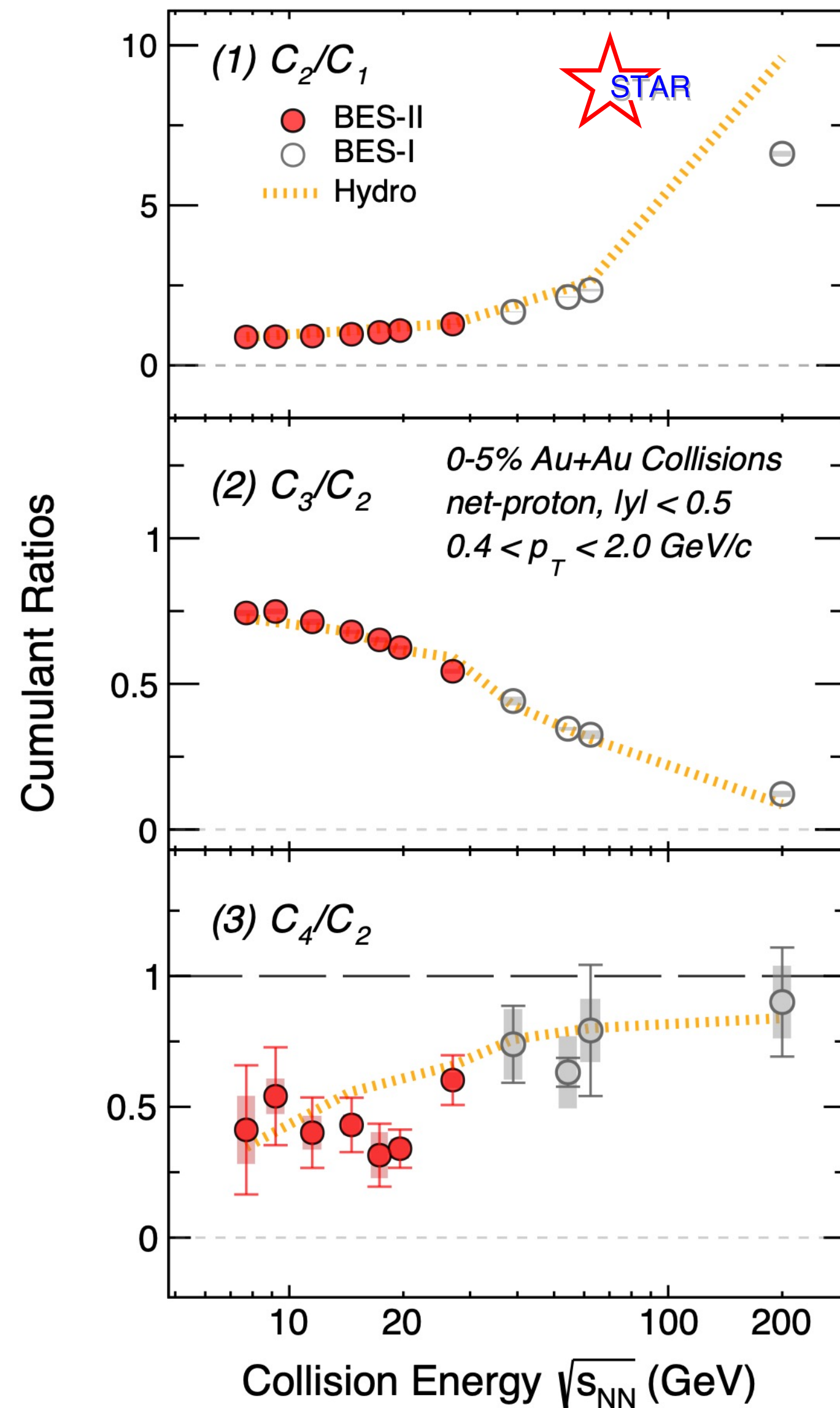
Net-proton cumulant ratios



- ◆ Smooth variation vs $\sqrt{s_{NN}}$ in C_2/C_1 and C_3/C_2 observed. C_4/C_2 decreases with decreasing energy.

Energy Dependence: Model Comparison

Net-proton cumulant ratios



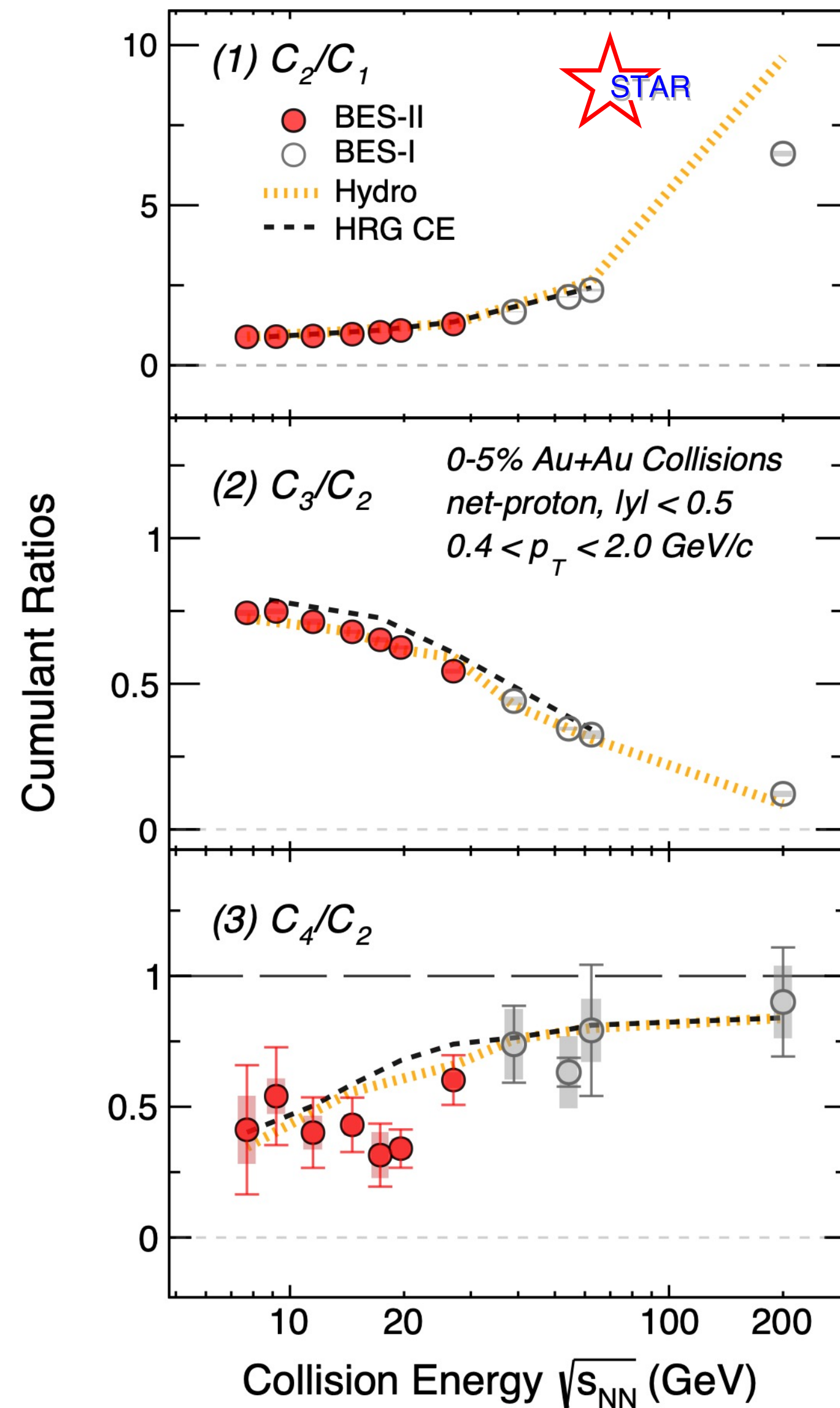
Smooth variation vs $\sqrt{s_{NN}}$ in C_2/C_1 and C_3/C_2 observed. C_4/C_2 decreases with decreasing energy.

Non-CP models used for comparison:
A. Hydro: Hydrodynamical model

V. Vovchenko et al, PRC 105, 014904 (2022)

Energy Dependence: Model Comparison

Net-proton cumulant ratios



◆ Smooth variation vs $\sqrt{s_{NN}}$ in C_2/C_1 and C_3/C_2 observed. C_4/C_2 decreases with decreasing energy.

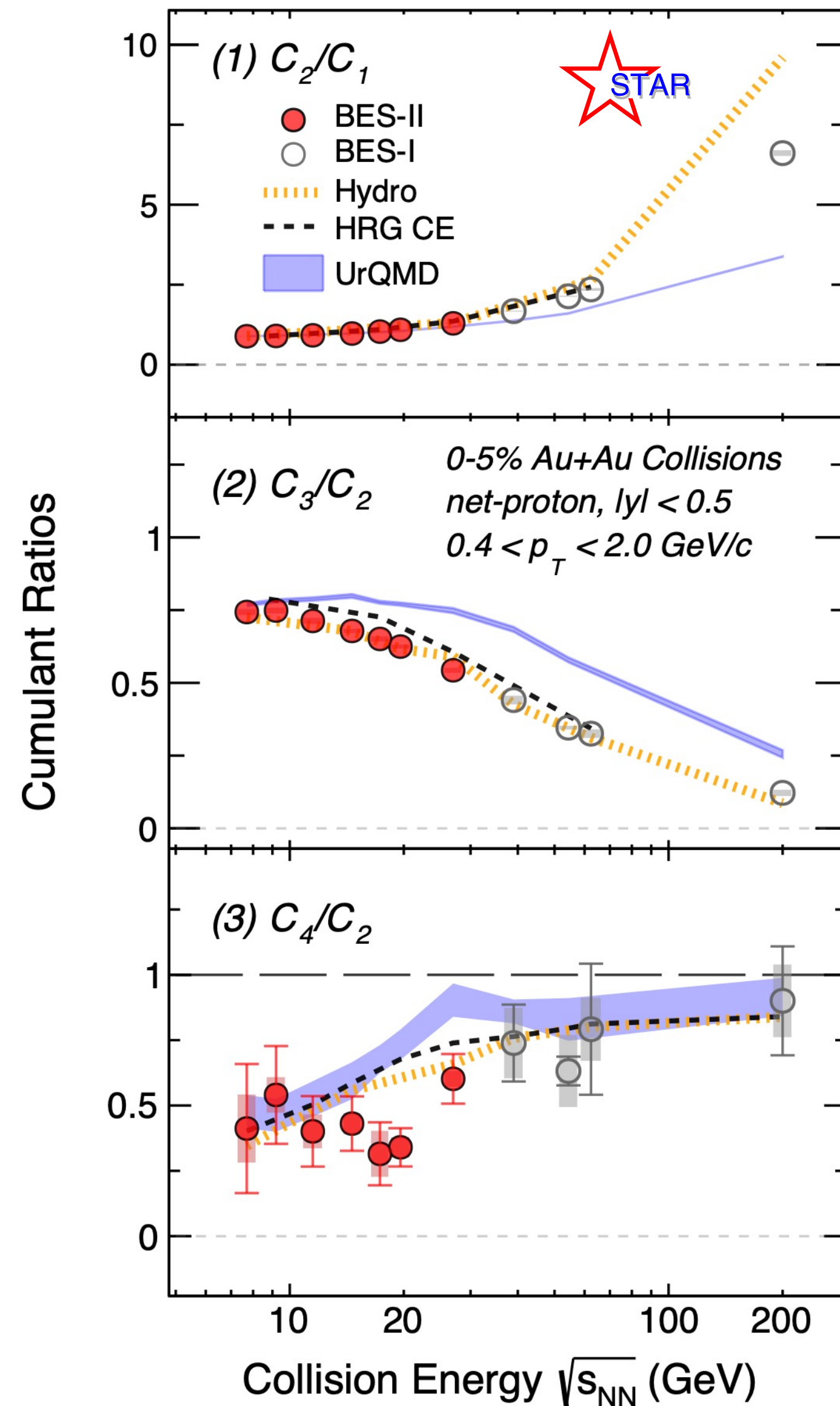
◆ Non-CP models used for comparison:
A. Hydro: Hydrodynamical model

V. Vovchenko et al, PRC 105, 014904 (2022)

B. HRG CE: Thermal model with canonical treatment of baryon charge *P. B Munzinger et al, NPA 1008, 122141 (2021)*

Energy Dependence: Model Comparison

Net-proton cumulant ratios



Smooth variation vs $\sqrt{s_{NN}}$ in C_2/C_1 and C_3/C_2 observed. C_4/C_2 decreases with decreasing energy.

Non-CP models used for comparison:
A. Hydro: Hydrodynamical model

V. Vovchenko et al, PRC 105, 014904 (2022)

B. HRG CE: Thermal model with canonical treatment of baryon charge

P. B Munzinger et al, NPA 1008, 122141 (2021)

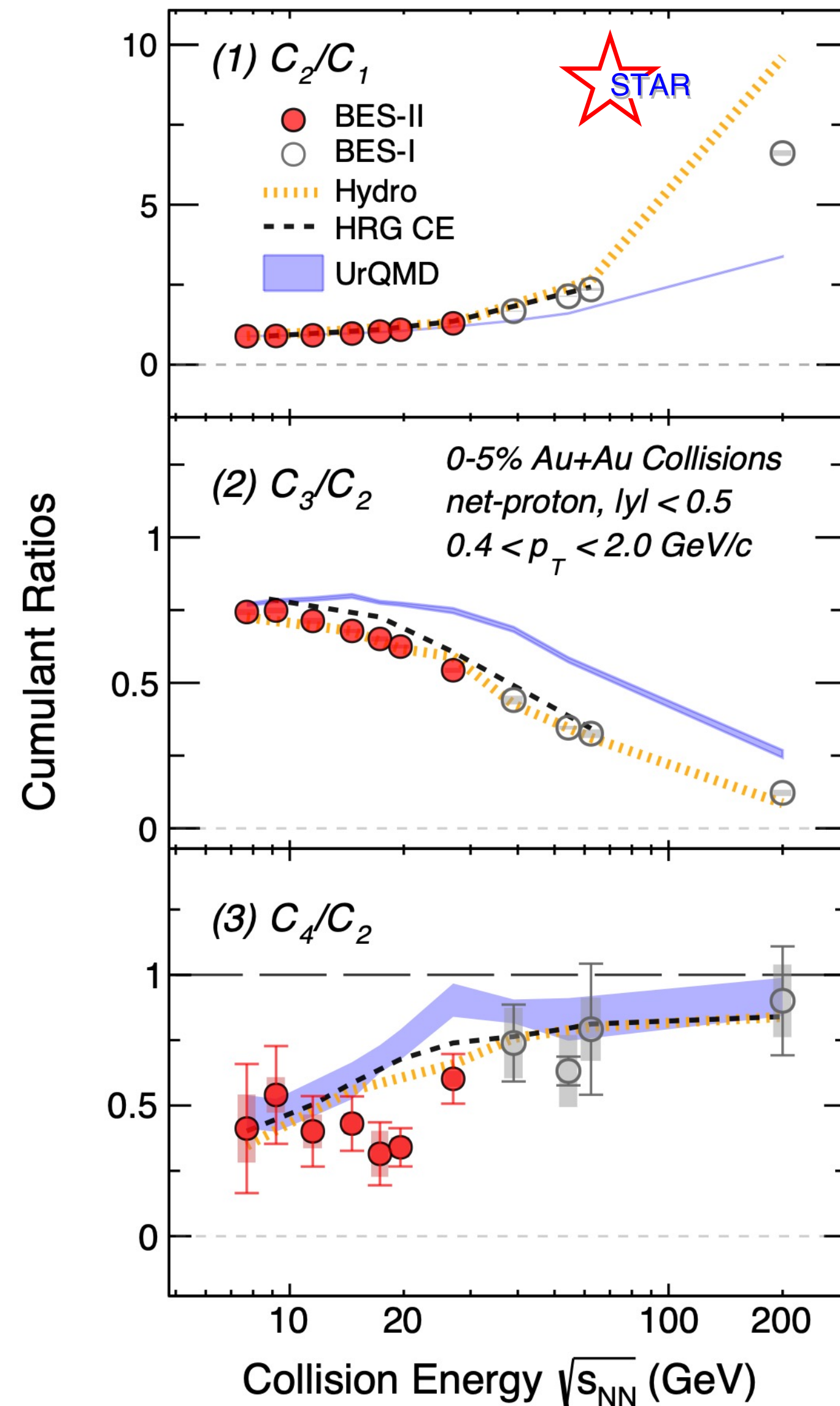
C. UrQMD: Hadronic transport model

Bass S., et al. Prog. Part. Nucl. Phys., 41, 255 (1998)

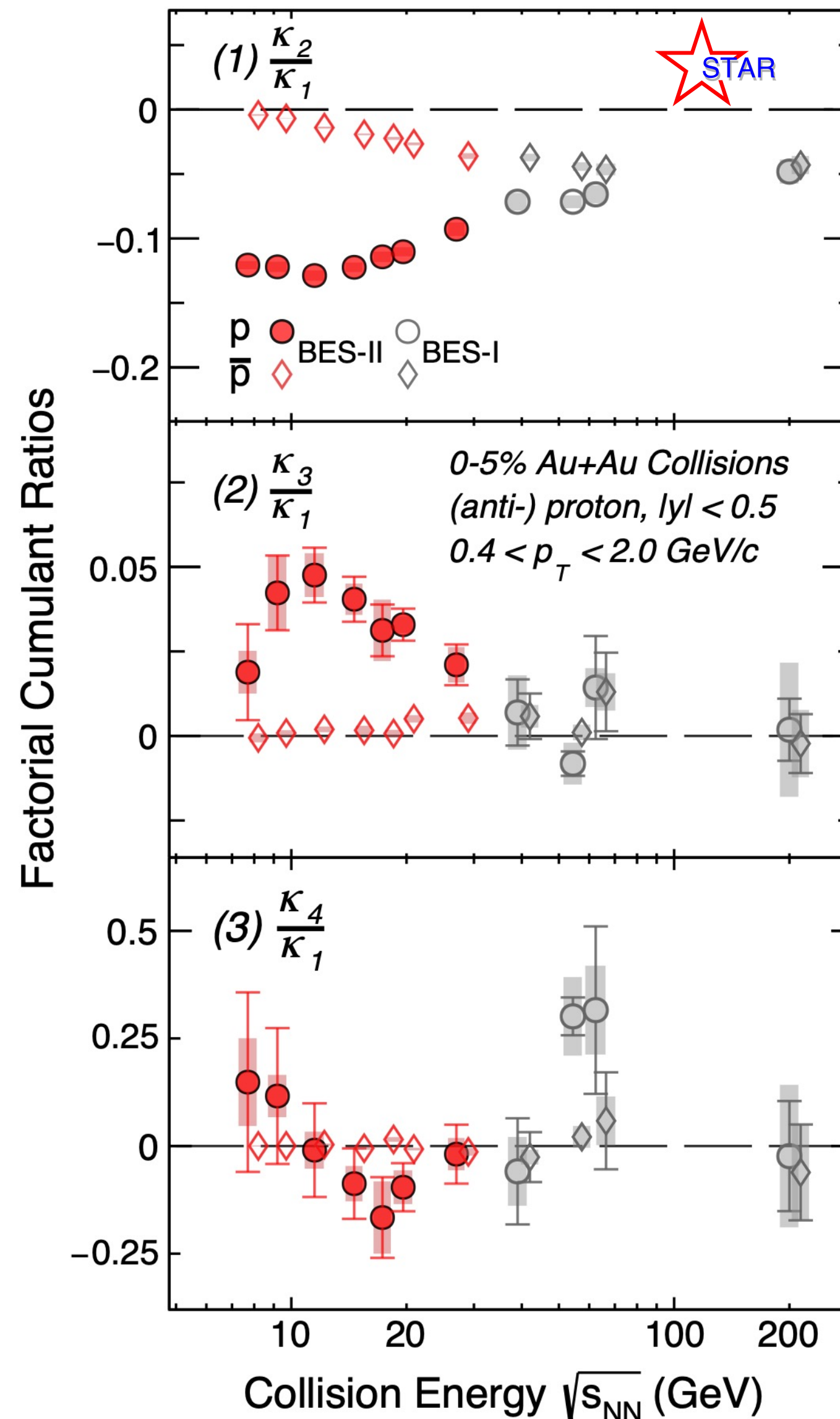
(All models include baryon number conservation)

Energy Dependence: Model Comparison

Net-proton cumulant ratios



(anti)proton factorial cumulant ratios



Smooth variation vs $\sqrt{s_{NN}}$ in C_2/C_1 and C_3/C_2 observed. C_4/C_2 decreases with decreasing energy.

Non-CP models used for comparison:
A. Hydro: Hydrodynamical model

V. Vovchenko et al, PRC 105, 014904 (2022)

B. HRG CE: Thermal model with canonical treatment of baryon charge

P. B. Munzinger et al, NPA 1008, 122141 (2021)

C. UrQMD: Hadronic transport model

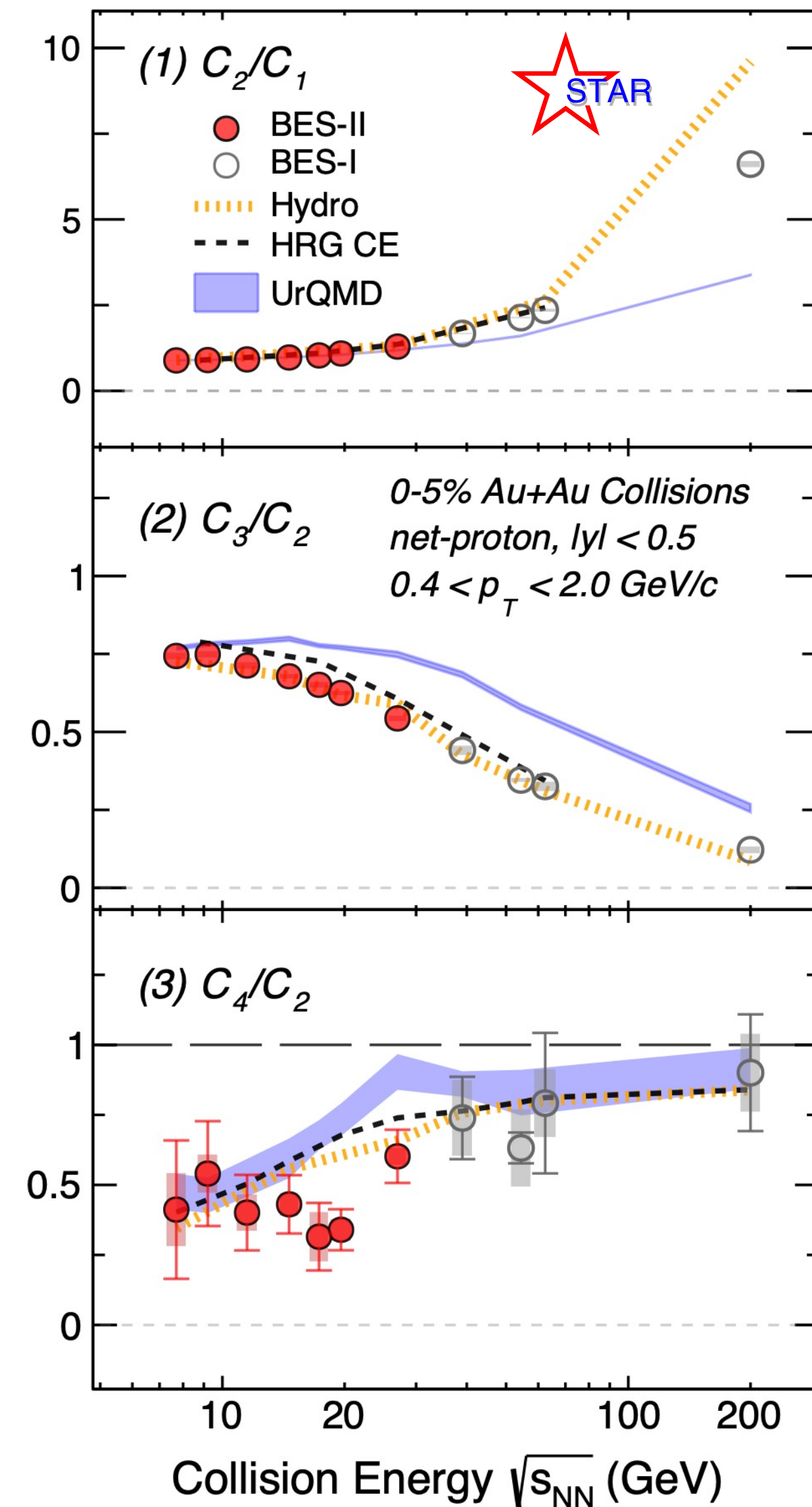
Bass S., et al. Prog. Part. Nucl. Phys., 41, 255 (1998)

(All models include baryon number conservation)

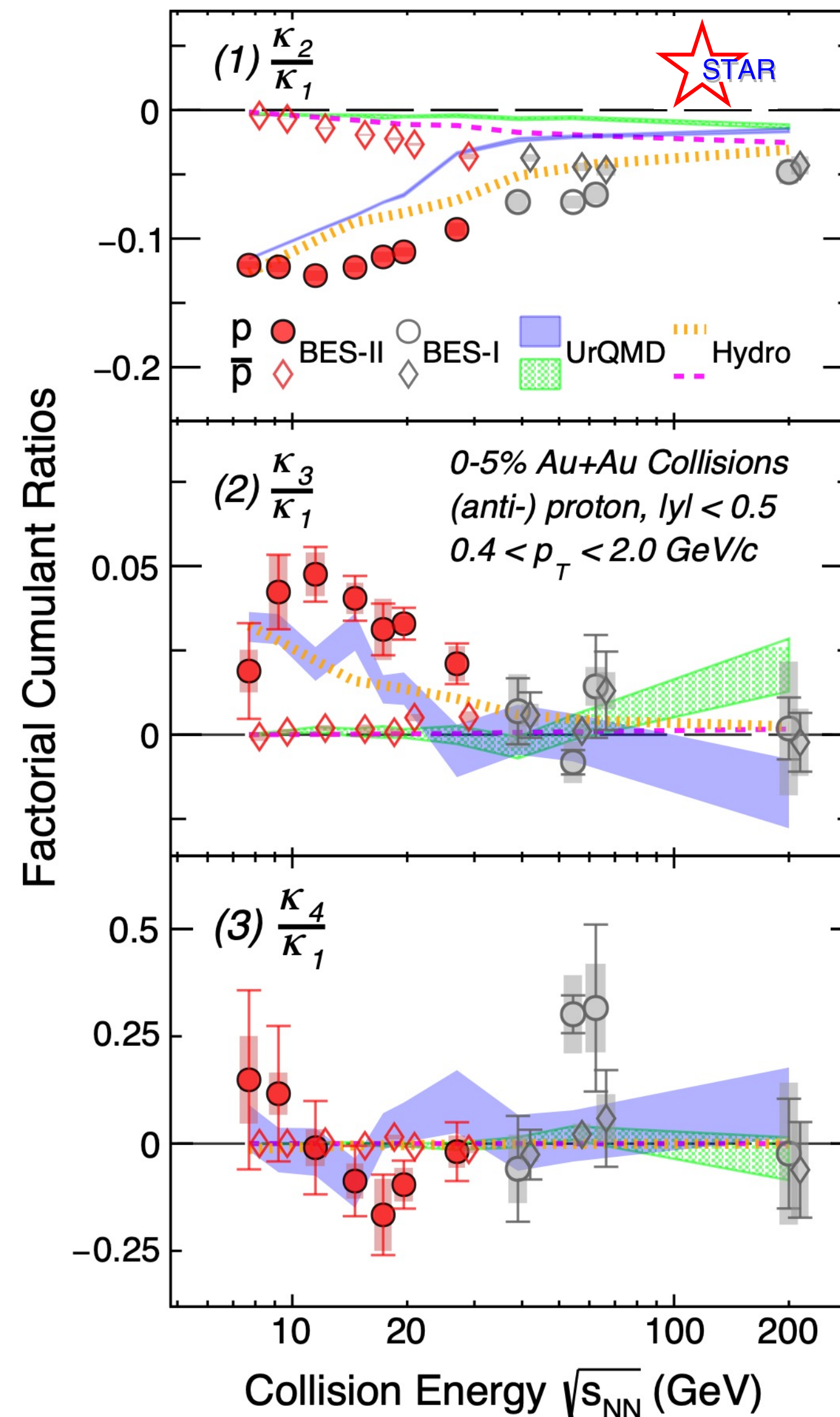
Proton factorial cumulant ratios deviates from Poisson baseline at 0.
Antiproton $\kappa_3/\kappa_1, \kappa_4/\kappa_1$ closer to 0.

Energy Dependence: Model Comparison

Net-proton cumulant ratios



(anti)proton factorial cumulant ratios



Smooth variation vs $\sqrt{s_{NN}}$ in C_2/C_1 and C_3/C_2 observed. C_4/C_2 decreases with decreasing energy.

Non-CP models used for comparison:
A. Hydro: Hydrodynamical model

V. Vovchenko et al, PRC 105, 014904 (2022)

B. HRG CE: Thermal model with canonical treatment of baryon charge

P. B. Munzinger et al, NPA 1008, 122141 (2021)

C. UrQMD: Hadronic transport model

Bass S., et al. Prog. Part. Nucl. Phys., 41, 255 (1998)

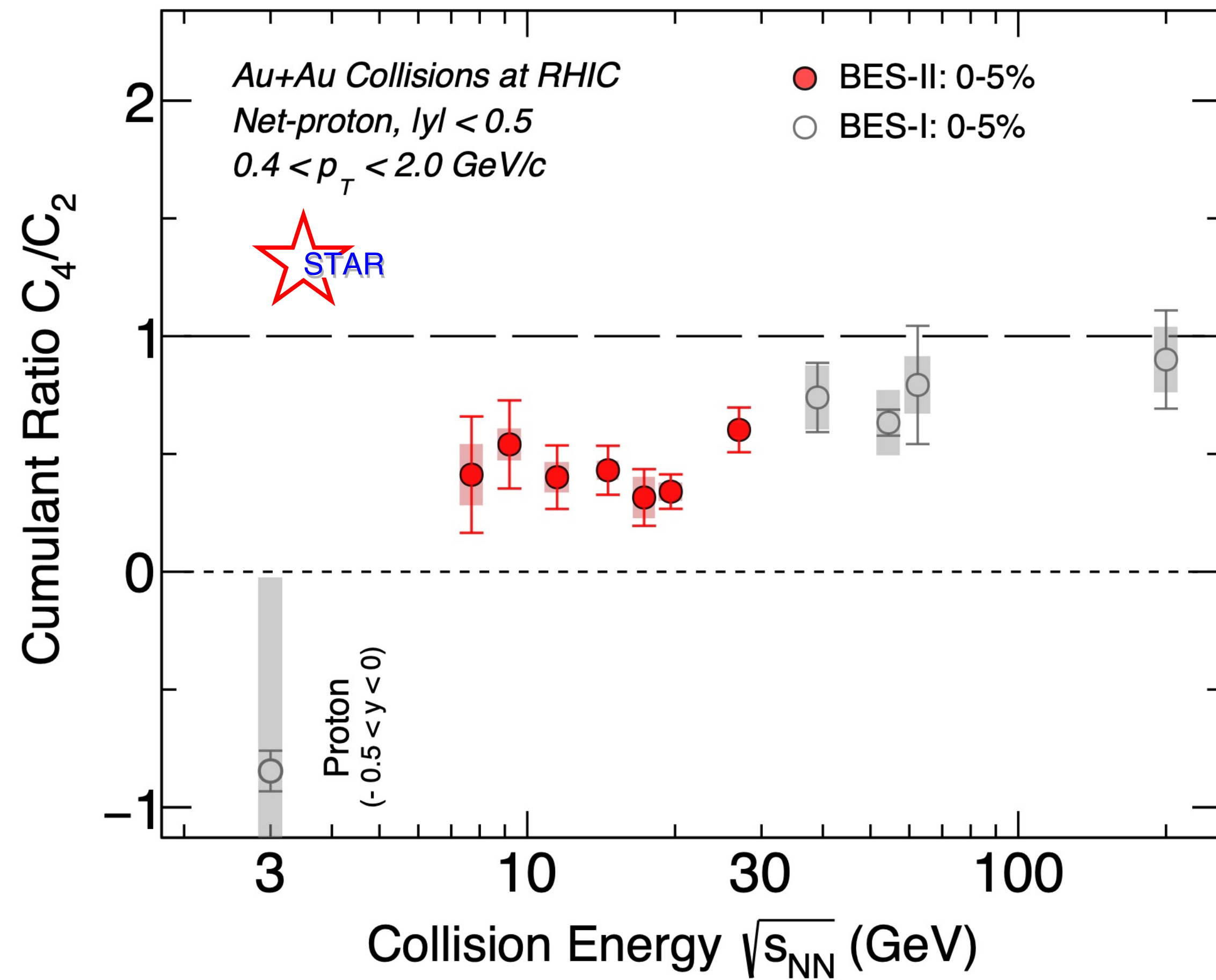
(All models include baryon number conservation)

Proton factorial cumulant ratios deviates from Poisson baseline at 0.

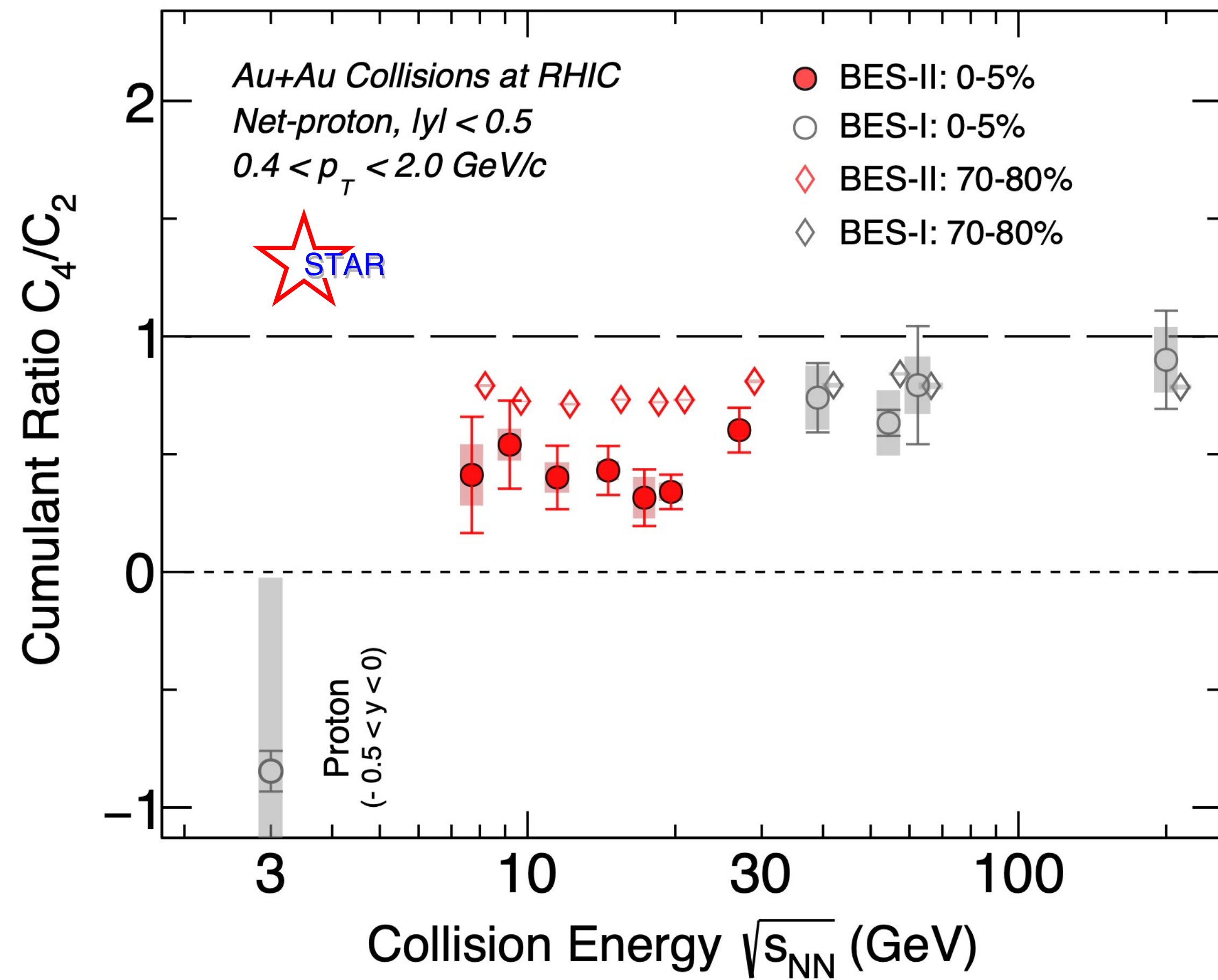
Antiproton $\kappa_3/\kappa_1, \kappa_4/\kappa_1$ closer to 0.

Baryon number conservation may shift the non-CEP model baseline but won't create criticality.

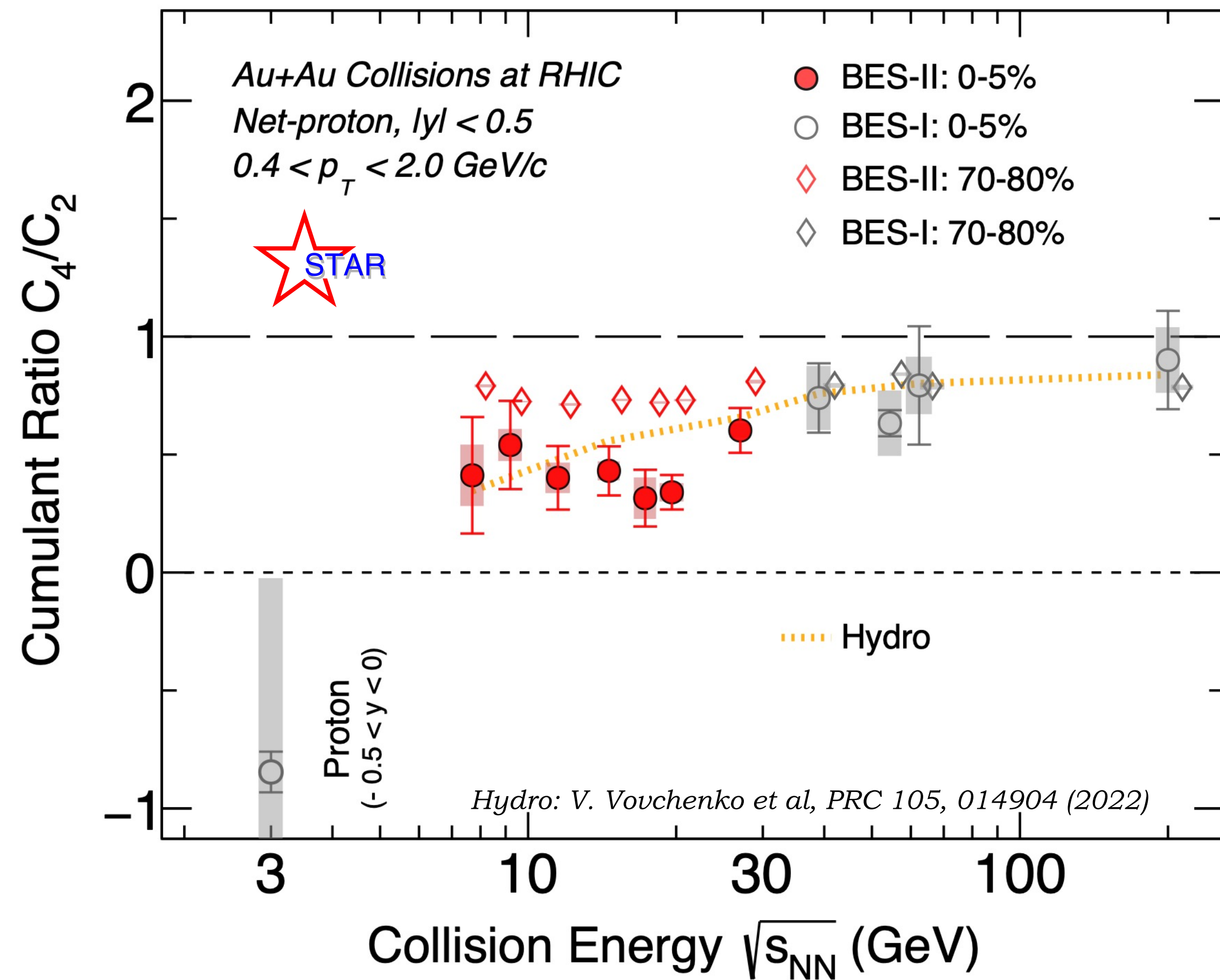
Energy Dependence of C_4/C_2



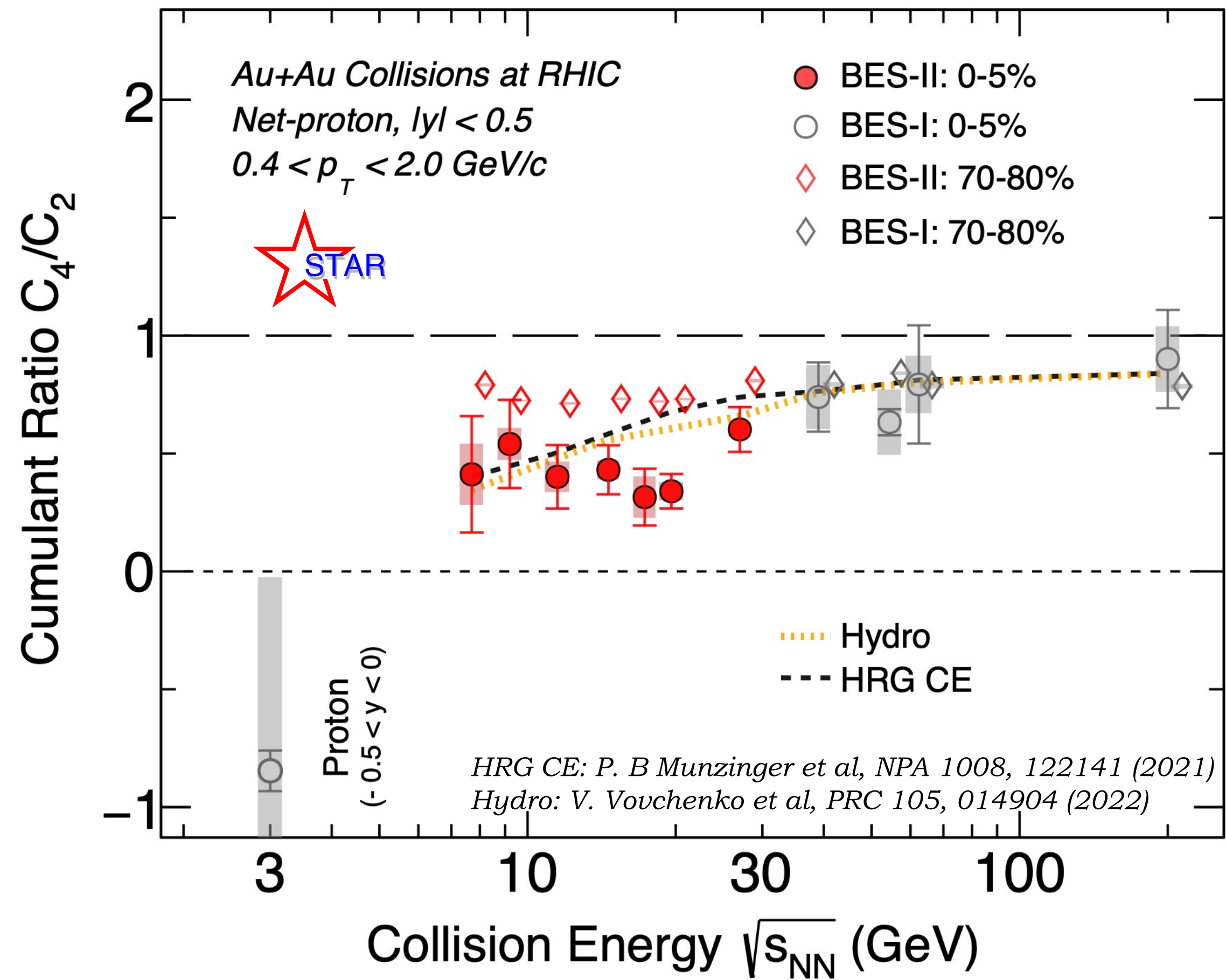
Energy Dependence of C_4/C_2



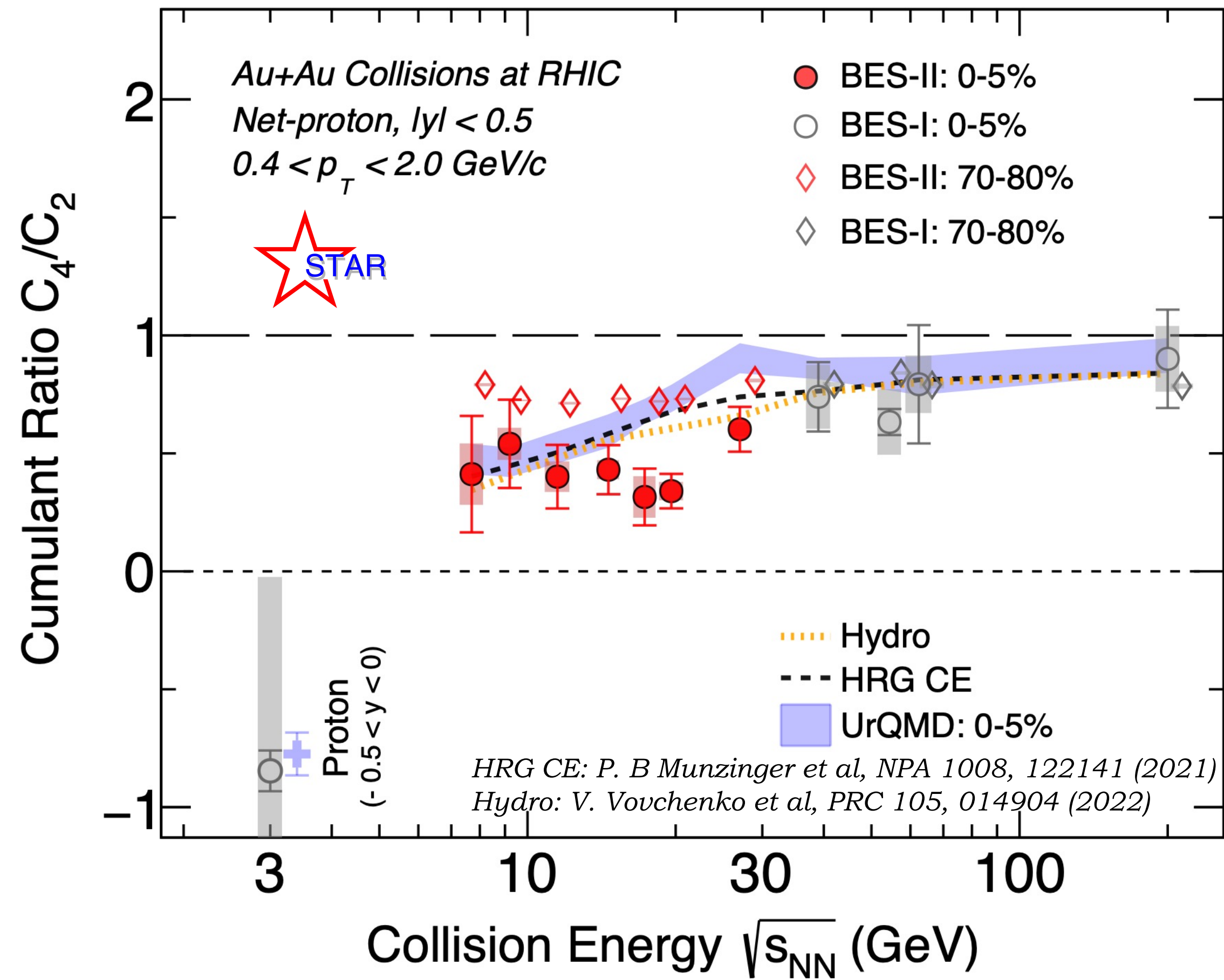
Energy Dependence of C_4/C_2



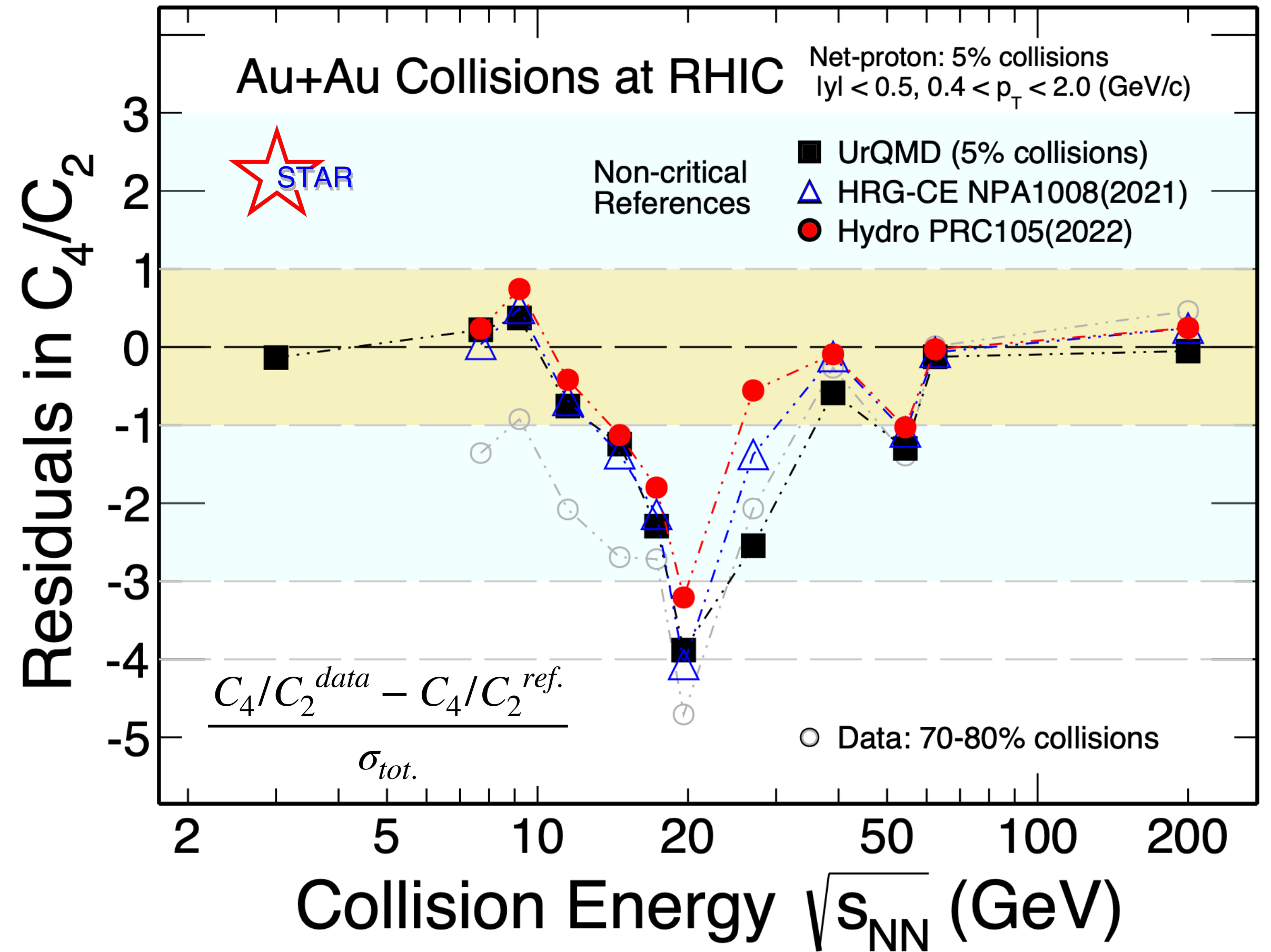
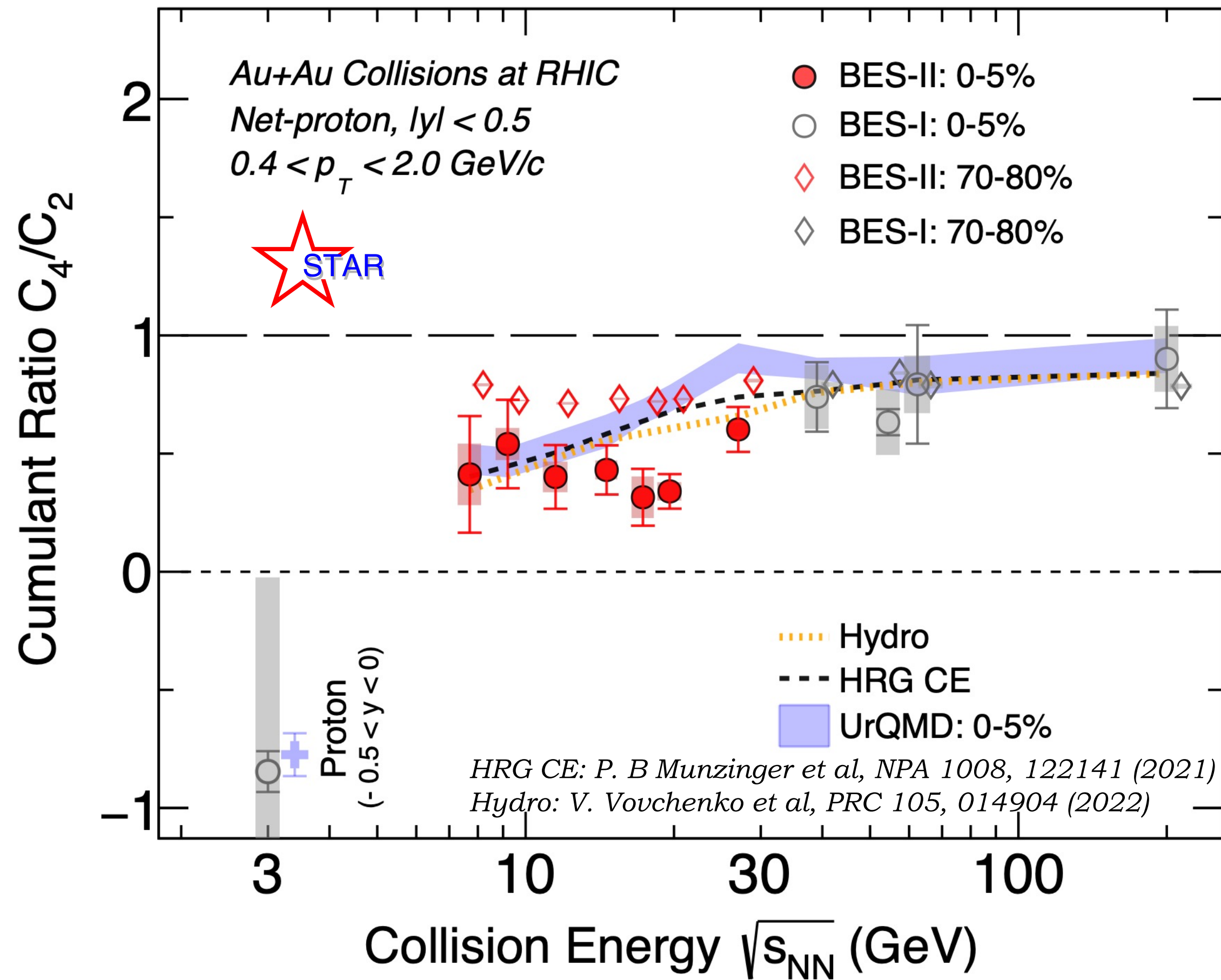
Energy Dependence of C_4/C_2



Energy Dependence of C_4/C_2

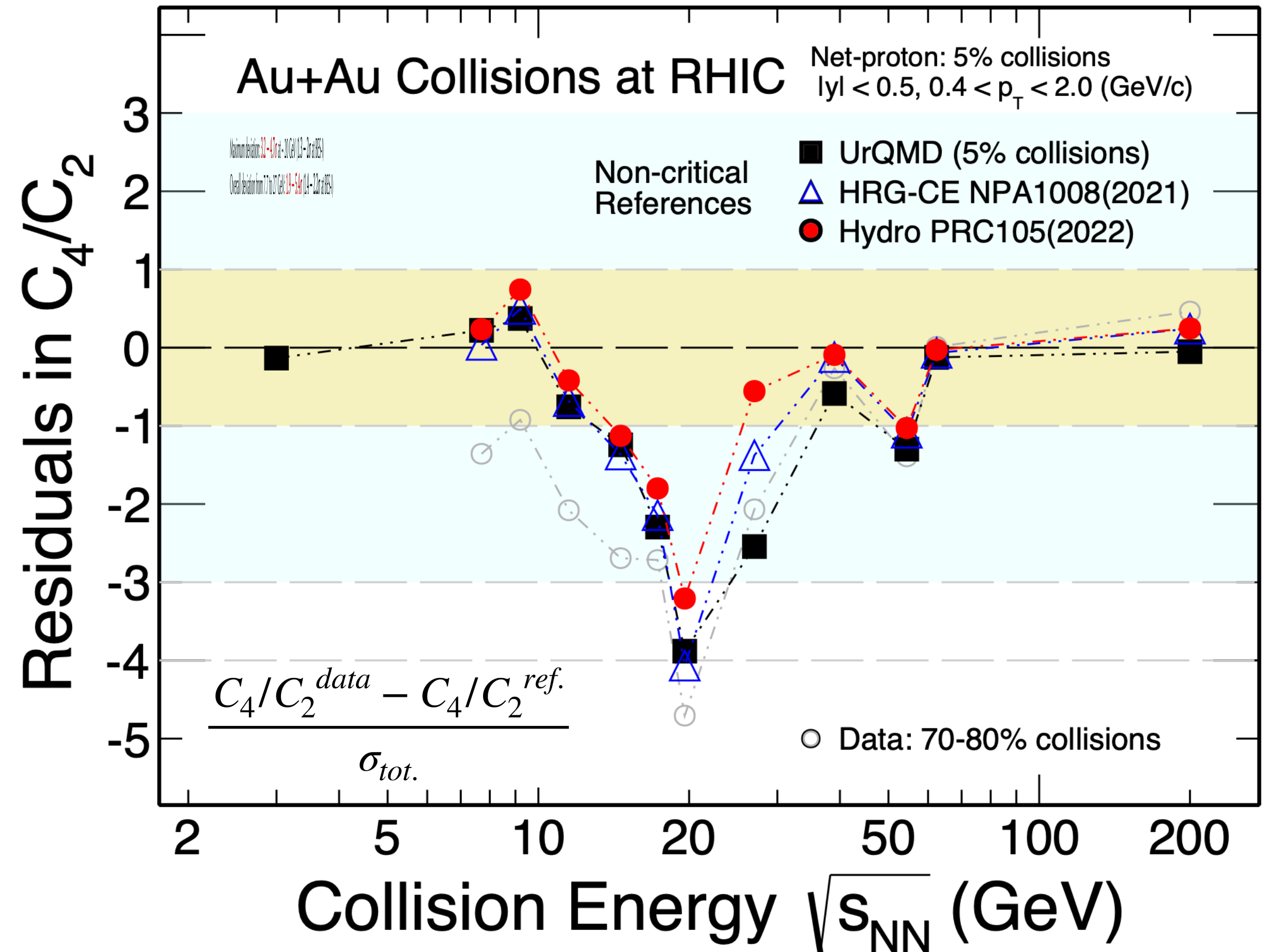
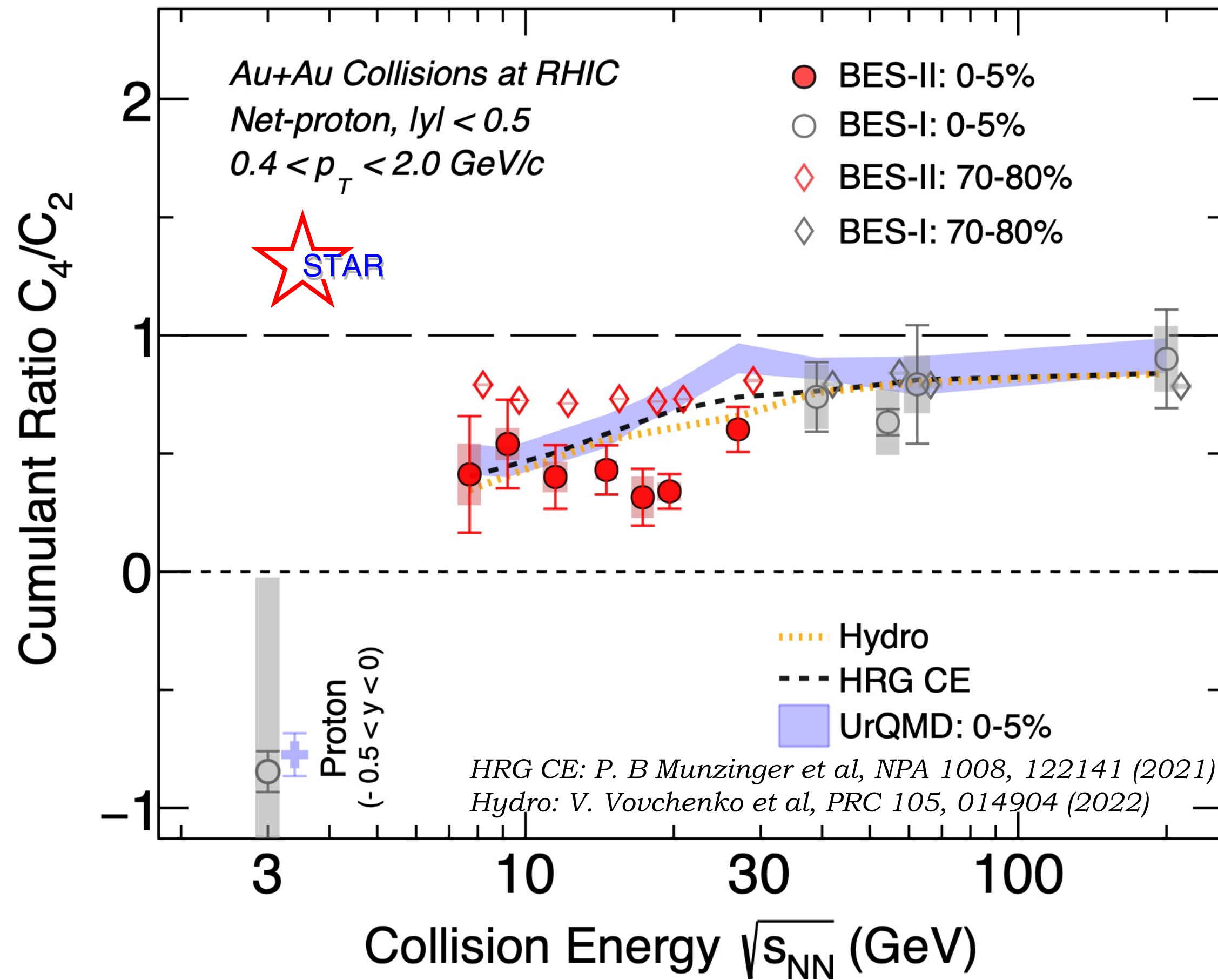


C_4/C_2 : Quantifying Deviation from Non-CP Models



C_4/C_2 shows minimum around ~ 20 GeV comparing to non-CEP models and 70-80% data.

C_4/C_2 : Quantifying Deviation from Non-CP Models



C_4/C_2 shows minimum around ~ 20 GeV comparing to non-CEP models and 70-80% data.

- ◆ Maximum deviation: $3.2 - 4.7\sigma$ at ~ 20 GeV ($1.3 - 2\sigma$ at BES-I)
- ◆ Overall deviation from 7.7 to 27 GeV: $1.9 - 5.4\sigma$ ($1.4 - 2.2\sigma$ at BES-I)

Summary and Outlook

Summary:

- ✦ Precision measurement of net-proton number fluctuations vs . centrality and collision energy in Au+Au collisions from STAR BES-II reported. Compared to BES-I, we have **better statistical precision, better centrality resolution, better control on systematics!**
- ✦ Net-proton C_4/C_2 in 0-5% central collisions show a maximum deviation w.r.t. various non-CP model calculations and 70-80% data is observed at $\sqrt{s_{NN}} = 20$ GeV with a significance level of **$3.2 - 4.7\sigma$** .

Outlook:

- ✦ Extend measurements to even higher orders of fluctuations: $C_n, \kappa_n (n = 1 - 6)$.
- ✦ Examine transverse momentum dependence and rapidity dependence of fluctuations.
- ✦ Complete the measurements in Au+Au collisions at fixed target (FXT) energies.



Acknowledgements

*RHIC operation for
successfully completing collection of BES-II data,*

*SQM2024 Organizers for
giving this opportunity.*

Thank you for your attention !

